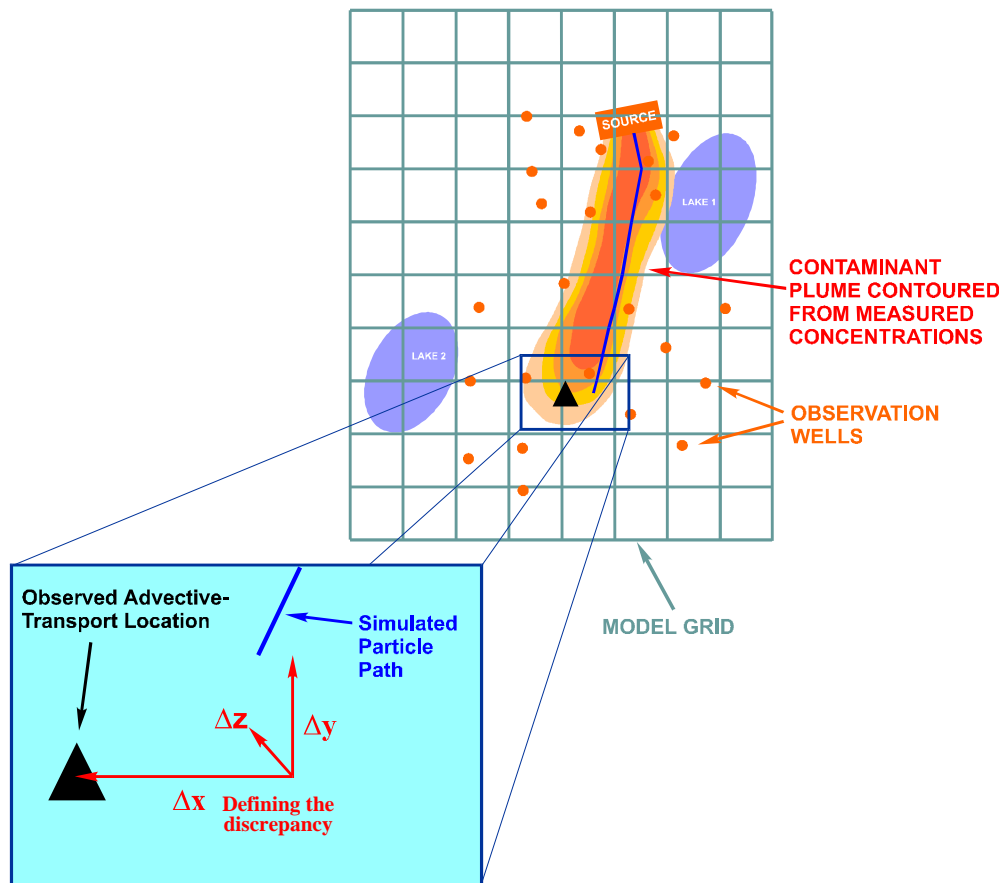# ADVECTIVE-TRANSPORT OBSERVATION (ADV) PACKAGE, A Computer Program for Adding Advective-Transport Observations of Steady-State Flow Fields to the Three-Dimensional Ground-Water Flow Parameter-Estimation Model MODFLOWP

Cover: Diagram showing conceptual representation of advective-transport observations (see Fig. 1 of this report)

ADVECTIVE-TRANSPORT OBSERVATION (ADV) PACKAGE,

A COMPUTER PROGRAM FOR ADDING ADVECTIVE-TRANSPORT OBSERVATIONS OF STEADY-STATE FLOW FIELDS TO THE THREE-DIMENSIONAL GROUND-WATER FLOW PARAMETER-ESTIMATION MODEL MODFLOWP

by Evan R. Anderman and Mary C. Hill

U.S. GEOLOGICAL SURVEY

Open-File Report 97-14

Denver, Colorado

1997

U.S. DEPARTMENT OF THE INTERIOR

BRUCE BABBITT, Secretary

U.S. GEOLOGICAL SURVEY

Gordon P. Eaton, Director

PREFACE

The computer program described in this report is designed to allow observations of the advective transport of steady-state ground-water flow through porous media to be used in the estimation of ground-water flow parameters. The program is developed as a package for the U.S. Geological Survey's MODFLOWP three-dimensional ground-water flow parameter-estimation model, and is intended to be the first of a family of alternative observation packages that can be used with MODFLOWP to estimate ground-water flow parameters and calibrate ground-water flow models.

The code for this model will be available for downloading over the Internet from a U.S. Geological Survey software repository. The repository is accessible on the World Wide Web from the U.S. Geological Survey Water Resources Information web page at URL http://water.usgs.gov/. The URL for the public repository is http://water.usgs.gov/software/. The repository is also available from a anonymous FTP site on the Water Resources Information server (water.usgs.gov or 130.11.50.175) in the /pub/software directory. When this code is revised or updated in the future, new versions or releases will be made available for downloading from these same sites.

ACKNOWLEDGMENTS

CONTENTS

FIGURES

TABLES

CONVERSION FACTORS

Multiply	By	To Obtain
cubic foot per second (ft^3/s)	0.3048	cubic meter per second (m^3/s)
foot (ft)	0.3048	meter (m)
foot per second (ft/s)	0.3048	meter per second (m/s)
inch (in)	25.4	millimeter (mm)
mile (mi)	1.609	kilometer (km)
square feet (ft^2)	0.0929	square meters (m^2)
square mile (mi^2)	2.59	square kilometer (km^2)

ADVECTIVE-TRANSPORT OBSERVATION (ADV) PACKAGE,

A COMPUTER PROGRAM FOR ADDING ADVECTIVE-TRANSPORT OBSERVATIONS OF

STEADY-STATE FLOW FIELDS TO THE THREE-DIMENSIONAL GROUND-WATER FLOW

PARAMETER-ESTIMATION MODEL MODFLOWP

by Evan R. Anderman and Mary C. Hill

ABSTRACT

Observations of the advective component of contaminant transport in steady-state flow fields can provide important information for the calibration of ground-water flow models. This report documents the ADV, Advective-Transport Observation, Package, which allows advective-transport observations to be used in conjunction with the hydraulic head and head-dependent flow observations included in the three-dimensional ground-water flow parameter-estimation model MODFLOWP.

The particle-tracking routine used in the ADV Package duplicates the semi-analytical method of MODPATH, as shown in a sample problem. Users are allowed to track particles in a forward or backward direction, or even to include effects such as retardation through manipulation of the effective-porosity value used to calculate velocity. Although effective porosity could be included as a parameter in the regression, this capability is not included in this package.

The weighted sum-of-squares objective function, which is minimized in the parameter estimation process, was augmented to include the square of the weighted x-, y-, and z-components of the differences between the simulated and observed advective-front locations at defined times, thereby including the direction of travel as well as the overall travel distance in the calibration process. The sensitivities of the particle movement to the parameters needed to minimize the objective function are calculated for any particle location using the exact sensitivity-equation approach; the equations are derived by taking the partial derivatives of the semi-analytical particle-tracking equation with respect to the parameters. The ADV Package is verified by showing that parameter estimation using advective-transport observations produces the true parameter values in a small but complicated test case when exact observations are used.

To demonstrate how the ADV Package can be used in practice, a field application is presented. In this application, the ADV Package is used to investigate the importance of advective-transport

observations relative to head-dependent flow observations when either or both are used in conjunction with hydraulic-head observations in a simulation of the sewage-discharge plume at Cape Cod, Massachusetts. The analysis procedure presented can be used in many circumstances to evaluate the probable effect of new observations on the parameter estimation. The procedure consists of two steps: (1) Parameter sensitivities and correlations calculated at initial parameter values are used to assess the model parameterization and expected relative contributions of different types of observations to the regression; and (2) optimal parameter values are estimated by nonlinear regression and evaluated. In this application, advective-transport observations improved the calibration of the model and the estimation of ground-water flow parameters, and use of formal parameter-estimation methods and related techniques produced significant insight into the physical system.

INTRODUCTION

The use of nonlinear regression to estimate optimal parameter values of ground-water flow models (Yeh, 1986; Carrera and Neuman, 1986a, b, and c; Cooley and Naff, 1990; Hill, 1992; Sun, 1994) results in more objective, automated, model calibration than using trial-and-error calibration methods alone, and allows for quantitative evaluation of model reliability. Simultaneously, use of nonlinear regression raises awareness of problems in ground-water flow model calibration that often are obscure when calibration is accomplished by trial and error alone. Such problems include (1) parameters important to the predictions for which the ground-water flow model is developed may not be precisely estimated because available observations provide insufficient information, (2) high correlation between parameters prevents them from being uniquely estimated using available observations, but the individual values may be important to predictions, and (3) different ground-water flow model constructions with optimal parameter estimates may fit the available observations equally well. Use of regression in the model calibration procedure makes these problems more obvious.

Historically, many ground-water flow models have been calibrated using only measurements of hydraulic head. The insensitivity and non-uniqueness that often occur when only head observations are used can be reduced by obtaining additional field observations, such as flow rate at head-dependent boundaries (Hill, 1992), temperature (Woodbury and Smith, 1988; Doussan and others, 1994), resistivity (Ahmed and others, 1988), or concentration (Strecker and Chu, 1986; Wagner and Gorelick, 1987; Sun and Yeh, 1990a and b; Keidser and Rosbjerg, 1991; Cheng and Yeh, 1992; Xiang and others, 1993;

Weiss and Smith, 1993; Sun, 1994; Harvey and Gorelick, 1995; Christiansen and others, 1995; Hyndman and Gorelick, 1996; Medina and Carrera, 1996; and others).

Using concentration data directly in the nonlinear regression is complicated by, among other things, the large computational effort required to solve the advective-dispersive equation. Partly because of this problem, parameter-estimation models that use concentration data directly are not widely used in practice, effectively limiting the calibration of ground-water flow model parameters to the use of head and flow data alone. It is apparent, therefore, that there is a need for innovative methods to extract fundamental ground-water flow system information from concentration data without resorting to use of the advective-dispersive equation.

An alternative approach to using concentration data directly is to derive observations of the advective component of solute transport from concentration data, and use these observations in the estimation of ground-water flow parameters. Observations of time and path of advective transport contain important information about ground-water flow parameters because they are a direct consequence of ground-water velocities and generally reflect more long-term aquifer conditions than head or flow observations.

It can be difficult to accurately locate the advective front of a contaminant plume directly from concentration data because of the effects of, for example, transverse dispersion and complex patterns of transport. Some of the difficulties are investigated in this report using synthetic test cases. Use of advective-transport observations in the estimation of ground-water flow parameters of field problems was considered by Sykes and Thomson (1988) and Anderman and others (1996). Both concluded that the advective-transport observations were important to model calibration.

Purpose and Scope

In this report, advective-transport observations are represented using the Advective-Transport Observation (ADV) Package of the three-dimensional ground-water flow parameter-estimation model MODFLOWP (Hill, 1992) using particle-tracking methods. The weighted sum-of-squares objective function of MODFLOWP is augmented to include the square of the weighted x-, y-, and z-components of the differences between the simulated and observed advective-front locations at defined times. This method expands on the work of Sykes and Thomson (1988) because it uses the position of advective transport as well as the overall travel time. The particle-tracking capabilities of the ADV module are evaluated using the sample problem presented in the MODPATH documentation (Pollock, 1989, p. 43).

3

Using advective-transport observations to estimate parameter values is evaluated in a small but complex synthetic test case. The use of advective-transport observations in a field problem is demonstrated through an application to the Otis Air Force Base sewage-discharge plume on Cape Cod, Massachusetts.

<u>Conceptual Approach</u>

The conceptual basis for the use of advective-transport observations is best illustrated through an example of a hypothetical field area, as shown in figure 1. At this site, the contaminant source has been active long enough to produce an extensive plume. A number of monitoring wells measure the extent of contaminated ground water, as well as the elevation of the water table. Additionally, the average annual amount of flow between one of the lakes and the ground-water system has also been measured. The sharp fronts of the concentration contours shown in figure 1 indicate that the movement of the contaminant plume is largely due to advection so that the direction and length of the plume are controlled by the hydrogeologic characteristics of the field site. Although the head and flow observations represent aquifer conditions at discrete points in time, the configuration of the contaminant plume represents average aquifer conditions integrated over the time of contaminant movement. An advective-transport observation can be obtained by contouring measured contaminant concentrations and choosing a suitable point along the plume front, as shown by the triangle in figure 1. The selection of the advective-front location is generally not straightforward, and is discussed in more detail in the OBTAINING ADVECTIVE-TRANSPORT OBSERVATIONS section. Once an observation is obtained, a simulated equivalent is needed. To simulate advective transport, a particle is tracked through the grid from the source location for the total time of contaminant transport, as shown by the gray line in figure 1. The differences in the x-, y-, and z-components between the simulated and observed advective-front locations are then used in the nonlinear regression in conjunction with the differences between the simulated and observed heads and flows to estimate model parameter values.

There are several conceptual advantages of particle tracking over the use of the full advective-dispersive equation. First, particle tracking is not affected by numerical dispersion, which hampers many advection-dispersion models. Second, the computational effort is greatly reduced because computations are only required along the particle path. Only a single particle usually needs to be tracked to represent the advective transport of each point source considered.

Particle tracking has at least two primary drawbacks. First, it is unclear how to locate the advective front of a contaminant plume moving in three dimensions in the presence of dispersion,

MODEL GRID

SOURCE

LAKE 1

LAKE 2

CONTAMINANT PLUME CONTOURED FROM MEASURED CONCENTRATIONS

OBSERVATION WELLS

Observed Advective-Transport Location

Simulated Particle Path

Δz

Δy

Δx
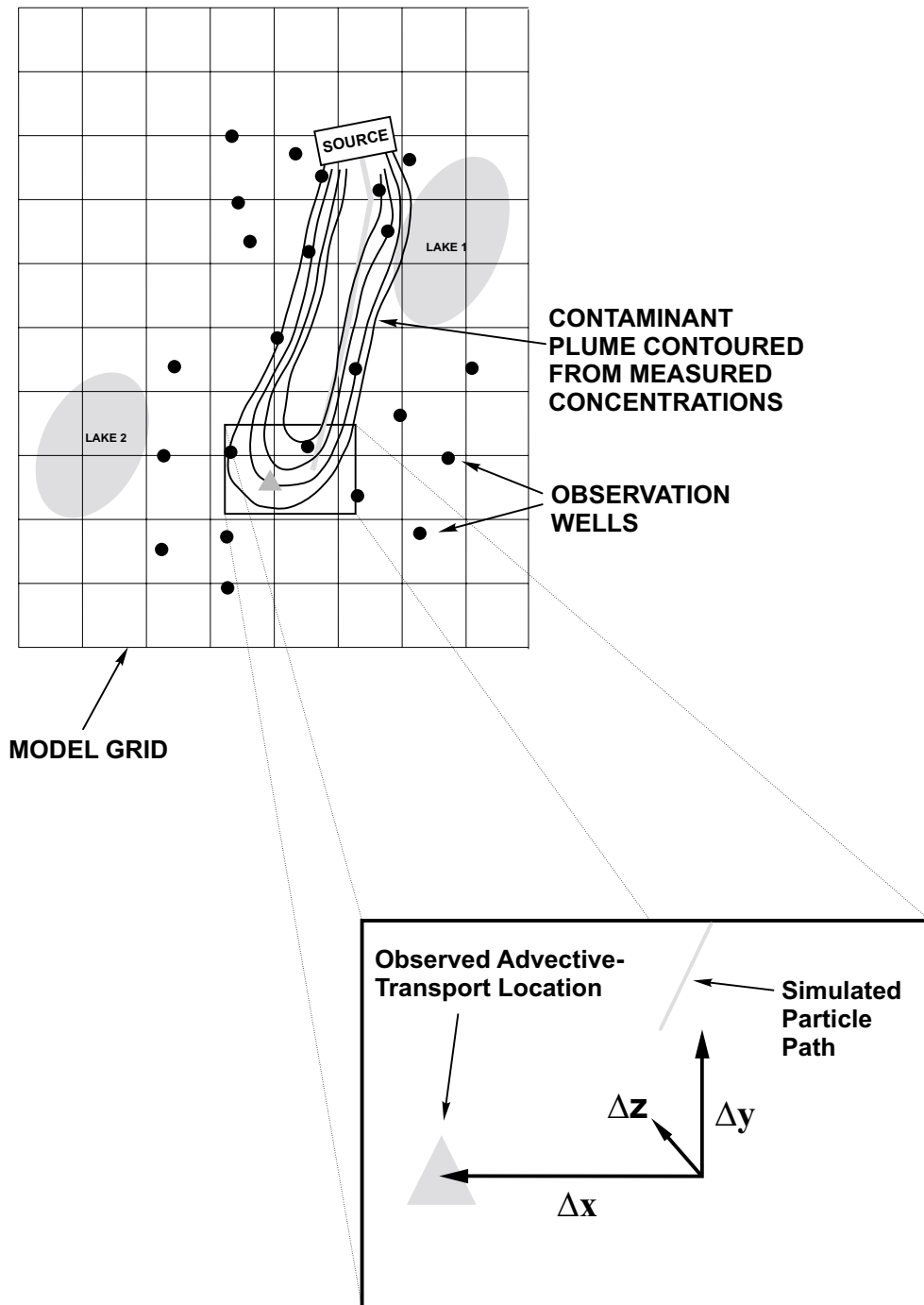
Figure 1.--Conceptual representation of advective-transport observations.

retardation, decay, chemical reactions, a possibly transient flow field, and other factors that cause solute transport in actual systems to differ from plug flow. In many instances, these problems are compounded by the absence of a reliable history of source release strengths, amounts, or locations. Some comments about these problems are presented in the OBTAINING ADVECTIVE-TRANSPORT OBSERVATIONS section. Even if the advective-transport location has been incorrectly identified, however, the flow model would still at least be calibrated with some consideration of the correct flow direction.

The second drawback to the use of particle tracking is that abrupt changes in hydraulic conductivity laterally or vertically can result in simulated flow paths that change dramatically as hydraulic conductivity changes (LaVenue and others, 1989; Poeter and Gaylord, 1990). These dramatic changes can violate smoothness requirements of gradient-based optimization methods, such as the modified Gauss-Newton method used in this work. An example of this problem is presented in the COMMON PROBLEMS section.

The method developed in this work is not restricted to representing the movement of a contaminant. The time and path of travel could be determined from a tracer test or from age dating of water samples that originate from a known location. The model presented here is applicable to these and many other situations, but is not applicable to situations in which the source or destination location is unspecified.

Methods

To incorporate particle tracking into the modified Gauss-Newton optimization method used in MODFLOWP (Hill, 1992, p. 76), the calculated particle location and its sensitivity to each estimated parameter are needed. Particle location is simulated by tracking the successive Cartesian (x-, y-, and z-) components of particle displacement through the ground-water flow model grid over time. Particle tracking was incorporated into the forward and inverse capabilities of MODFLOWP for particles moved by steady-state simulated flow. Particle-tracking computations are only required to determine the path of a single particle for each observation, greatly reducing the computational effort compared to solution of the advective-dispersive equation. The particle-tracking method used is the semi-analytical method presented by Pollock (1989) modified so that the cell-face velocities are calculated using an interpolated saturated thickness, instead of the single-cell saturated thickness used in MODPATH. The original method produces discontinuities in velocity, and thus sensitivity, at cell boundaries. The velocity at any point within a cell is linearly interpolated from cell-face velocities. Users are allowed to track particles

in a backward direction, and manipulation of the effective-porosity value needed to calculate velocity allows effects such as retardation to be simulated. Given an initial particle position, the x-, y-, and z-displacements are calculated and a single particle is tracked through the model grid for a specified amount of time. The sensitivities of the particle movement to the parameters are calculated for any particle location using the exact sensitivity-equation approach, which is consistent with the sensitivity calculations in MODFLOWP, by taking the partial derivatives of the semi-analytical particle-tracking equation with respect to the parameters.

ADVECTIVE-TRANSPORT OBSERVATION PACKAGE
METHODOLOGY

This section describes how the ADV Package interacts with MODFLOWP to incorporate advective-transport observations in the parameter estimation. The discussion includes the complete derivation of the augmented weighted sum-of-squares objective function, a brief description of how sensitivities are calculated, and a brief description of the forward particle-tracking equations used in the ADV Package; complete derivations of the particle-tracking equations and sensitivities are presented in Appendix C.

Augmented Objective Function and Normal Equations and The Calculation of Sensitivities

The ADV Package augments arrays in MODFLOWP that already contain observed and simulated hydraulic heads and flows and calculated sensitivities. In this way, the weighted sum-of-squares objective function in MODFLOWP is augmented to include the square of the weighted x-, y-, and z-components of the difference between the simulated and observed advective-front location at defined times. The sum-of-squares objective function, S, is then expressed as:

$$S = S_h + S_f + S_p + S_t \tag{1}$$

where

S_h is the sum of the squared weighted hydraulic-head differences,
S_f is the sum of the squared weighted head-dependent flow differences,
S_p is the sum of the squared weighted prior-information differences,
S_t is the sum of the squared weighted advective-transport differences, expressed as

$$\sum_{i=1}^{NT} \omega_i \left(x_i - \hat{x}_i \right)^2 + \upsilon_i \left(y_i - \hat{y}_i \right)^2 + \tau_i \left(z_i - \hat{z}_i \right)^2 \tag{1a}$$

where

NT   is the number of advective-transport observations,

x_i, y_i, z_i are the x-, y-, and z-components of the observed advective transport,

$\hat{x}_i$, $\hat{y}_i$, $\hat{z}_i$ are the x-, y-, and z-components of the simulated advective transport, and

ω_i υ_i τ_i are the x-, y-, and z- advective-transport observation weights.

The above expression for S_t is applicable when the weight matrix is diagonal, so that covariances between measurement errors are ignored. Although this is common in practice, the ADV Package supports a full weight matrix, as discussed in Appendix A. While errors in the x-, y-, and z-advective-transport movements are probably not independent, it is not clear how to determine error correlation, and few users are expected to use a full weight matrix. In the following discussion a diagonal weight matrix is assumed.

Determination of proper weighting is nearly always problematic. Linear theory indicates that parameter estimates with the smallest variances are achieved when the weights of equation (1a) equal the inverses of variances of the observation measurement error (Graybill, 1976; Draper and Smith, 1981, p. 110; Hill, 1992), and the authors have found this to be a useful guideline in nonlinear problems as well. Standard deviations and coefficients of variation are more intuitive to work with and can be used to calculate variances as the square of the product of the coefficient of variation and the measured value, or the square of the standard deviation. Many components of the measurement error can be difficult to quantify; for example, errors due to partially penetrating observation wells or the presence of residual drawdown from aquifer pumping are often inadvertently neglected. Thus, the specified error variances are often subjective and can be smaller than they should be. The tendency to be too small is reflected in the model fit, as measured by the calculated error variance or the standard error being greater than 1.0.

The minimum of the objective function in equation (1) is determined using the modified Gauss-Newton nonlinear optimization procedure presented by Hill (1992, p. 76):

$$\left(\underline{\underline{C}}^T \left(\underline{\underline{X}}_r^T \underline{\hat{\omega}} \underline{\underline{X}}_r + \underline{\underline{R}} \right) \underline{\underline{C}} + \underline{\underline{I}} \mu_r \right) \underline{\underline{C}}^{-1} \underline{d}_r = \underline{\underline{C}}^T \underline{\underline{X}}_r^T \underline{\hat{\omega}} \left(\underline{y} - \underline{\hat{y}}_r \right)$$
$$\underline{b}_{r+1} = \underline{b}_r + \rho_r \underline{d}_r \tag{2}$$

where

$\underline{\underline{C}}$ is a diagonal scaling matrix with elements equal to

$$C_{ii} = \left(\underline{\underline{X}}_r^T \hat{\underline{\underline{\omega}}} \underline{\underline{X}}_r \right)_{ii}^{-1/2}; \quad C_{ij} = 0 \quad i \neq j$$

$\underline{\underline{X}}_r$ is the sensitivity matrix evaluated at parameter values $\underline{b}_r$, with column j equal to

$\delta\hat{\underline{y}}_r \Big/ \delta b_j$, where b_j is an element of $\underline{b}_r$.

   r is the parameter-estimation iteration number,

$\hat{\underline{\underline{\omega}}}$ is the weight matrix,

$\underline{\underline{R}}$ can be included for problems with large residuals and a large degree of nonlinearity (see Hill, 1992, p. 77),

$\underline{\underline{I}}$ is the identity matrix, with elements equal to 1 along the diagonal and zero elsewhere,

$\underline{y}$ is the vector of observed values, such as heads, flows, and prior information,

$\hat{\underline{y}}_r$ is the vector of corresponding simulated values,

$\underline{d}_r$ is the vector used to update the parameter estimates,

μ_r is the Marquardt parameter,

ρ_r is the damping parameter, and

  T superscripted indicates the transpose of the vector or matrix.

To include advective-transport observations in the parameter estimation $\underline{y}$, $\hat{\underline{y}}_r$, $\hat{\underline{\underline{\omega}}}$, and $\underline{\underline{X}}_r$ of

the normal equations are augmented as follows. The advective-transport observation values are added to

the observation vector $\underline{y}$, which becomes:

$$\underline{y} = \begin{pmatrix} y_1 \\ \cdot \\ \cdot \\ \cdot \\ y_{nh} \\ y_{nh+1} \\ \cdot \\ \cdot \\ y_{nh+nq} \\ y_{nh+nq+1} \\ \cdot \\ \cdot \\ y_{nh+nq+nt*ktdim} \end{pmatrix} \qquad\qquad (3)$$

where

      nh is the number of head observations,

      nq is the number of flow observations,

      nt is the number of advective-transport observations, and

ktdim   is the dimension of the particle tracking, either 2 or 3.

The corresponding simulated values are calculated using the particle-tracking equations of the following sections and are added to the simulated-value vector $\hat{\underline{y}}_r$ at each parameter-estimation iteration. Thus, $\hat{\underline{y}}_r$ looks similar to $\underline{y}$ of equation (3) except that the elements are simulated instead of observed values. The weights of each of the advective-transport observations are added to the weight matrix $\hat{\underline{\underline{\omega}}}$. Thus, the augmented $\hat{\underline{\underline{\omega}}}$ is a nh+nq+nt*ktdim dimensional square matrix of the form shown by Hill (1992, p. 54). The sensitivity matrix $\underline{\underline{X}}_r$ is augmented with the sensitivity of each of the advective-transport observations i to each parameter j. The parameter vector $\underline{b}_r$ remains unchanged.

Calculation of sensitivities is the most computationally intensive part of nonlinear regression. Depending on the optimization method used to solve the nonlinear regression, there are more and less efficient methods to numerically calculate the sensitivities. The sensitivity-equation method (Yeh, 1986) is most efficient when the number of observations exceeds the number of estimated parameters. It is one of two methods available in MODFLOWP (Hill, 1992, p. 90), and is the only method supported by the ADV Package. Sensitivity-equation sensitivities are derived by taking the partial derivative of the governing equation with respect to each parameter, as discussed in Appendix C.

Calculation of Particle Location

Particle location is simulated by tracking the successive Cartesian (x, y, z) components of particle displacement through the ground-water flow model grid either forward or backward in time. The derivations of the particle-tracking equations are given in Appendix C for the x-component only; extension to the y- and z-components is straightforward. Vertical particle displacement is corrected for distorted grids using the methods of Pollock (1989, p. 12) and Zheng (1994). If the particle is discharged from the model grid before the time of the observation, the final simulated particle position is determined by projecting the particle using the velocities calculated at the point of discharge. Such projection of the final particle position often results in large advective-transport differences in equation 1, in effect penalizing unrealistic simulated advective-front positions.

Particles can be tracked in a backward direction in the ADV Package, a feature which has many uses in parameter estimation. For example, if the age of water at one point in the system and the likely

source area are known, this feature can be used to represent such an observation. Additionally, this feature can be used to calculate predicted well capture areas and the corresponding confidence intervals.

There are a number of special cases with respect to the calculation of the vertical velocities that are worth discussing here. A nonzero vertical velocity at the top of the top layer can only occur if there is an appropriate boundary condition active in the cell. In MODFLOW, a number of different types of boundaries, such as recharge, head-dependent boundaries (River, Streamflow-Routing, Drain, and General-Head Boundary Packages), and evapotranspiration, may contribute to the net flux at the top boundary. Conceptually, boundaries may represent sources of water which overlie, are adjacent to, or underlie the ground-water system being represented. It is not necessary to distinguish these special cases in MODFLOW; however, the different conceptual representations of boundaries are important to particle tracking (Pollock, 1989, p. 15). The ADV Package supports a more limited representation of boundary flows than is available in MODPATH. In the ADV Package, influx from boundary conditions that are applied to the top layer are assumed to apply to the top of the top layer. All other boundaries are considered as internal sources of water, so that the flow is introduced at the cell center.

The finite-difference approximation equations upon which the MODFLOW model is based assume that hydraulic properties are uniform within individual cells, or at least that average or integrated parameters can be specified for every cell (McDonald and Harbaugh, 1988, p. 2-31). Hydraulic head is calculated at cell centers, so that hydraulic properties of adjacent cells need to be combined to calculate conductances to be used in the continuity equation. This is accomplished within MODFLOW (McDonald and Harbaugh, 1988, p. 5-6 and 5-9) and BCF2 (McDonald and others, 1992, p. 5) for horizontal-conductance components within layers, but the calculation of vertical hydraulic conductance between layers is left to the user (McDonald and Harbaugh, 1988, p. 5-11). This conductance, called Vcont, is then used to calculate the flux between two layers using the head difference across the layer. There are three different configurations that Vcont could represent (fig. 2): (a) vertically adjacent cells span a single geohydrologic unit and both cells are assigned the same hydraulic conductivity; (b) vertically adjacent cells are assigned different hydraulic conductivity but no confining unit separate the two; or (c) vertically adjacent cells are assigned either the same or different hydraulic conductivity and a confining layer separates the two layers. The particle-tracking algorithm presented here is capable of tracking particles through model layers representing all of these situations. If situation (c) applies, however, then it is assumed that flow through the confining unit is vertical, and the thickness and effective porosity of the confining layer are needed to calculate the travel time through the confining layer (fig. 3).

Vertically Adjacent Geohydrologic Units

Geohydrologic Unit A

Geohydrologic Unit B

$K_{z\,i,j,k}$

$K_{z\,i,j,k+1}$

$h_{i,j,k}$

$h_{i,j,k+1}$

Δc_i

Δr_j

$l_{i,j,k}$

$l_{i,j,k+1}$

Boundary between model layers (coincident with geohydrologic boundary)

$$Vcont_{i,j,k+1/2} = \cfrac{1}{\cfrac{l_{i,j,k}}{2\,K_{z\,i,j,k}} + \cfrac{l_{i,j,k+1}}{2\,K_{z\,i,j,k+1}}}$$

Vertically Adjacent Geohydrologic Units Separated by a Confining Unit

Geohydrologic Unit A

Confining Unit

Geohydrologic Unit B

$K_{z\,i,j,k}$

$K_{z\,i,j,k}$

$K_{z\,i,j,k+1}$

$h_{i,j,k}$

$h_{i,j,k+1}$

Δc_i

Δr_j

$l_{i,j,k}$

$l_{i,j,k+1/2}$

$l_{i,j,k+1}$

$$Vcont_{i,j,k+1/2} = \cfrac{1}{\cfrac{l_{i,j,k}}{2\,K_{z\,i,j,k}} + \cfrac{l_{i,j,k+1/2}}{K_{zc}} + \cfrac{l_{i,j,k+1}}{2\,K_{z\,i,j,k+1}}}$$

Single Geohydrologic Unit

$h_{i,j,k}$

$h_{i,j,k+1}$

Δc_i

Δr_j

$l_{i,j,k}$

$l_{i,j,k+1}$

Boundary between model layers

$$Vcont_{i,j,k+1/2} = \frac{2\,K_{z_{i,j}}}{l_{i,j,k} + l_{i,j,k+1}}$$

Figure 2.-- Vertical discretization used in MODFLOWP (after McDonald and Harbaugh, 1988).

12

Model layer k

$h_{i,j,k}$

PARTICLE PATH

Semi-confining Unit

$l_{i,j,k+1/2}$
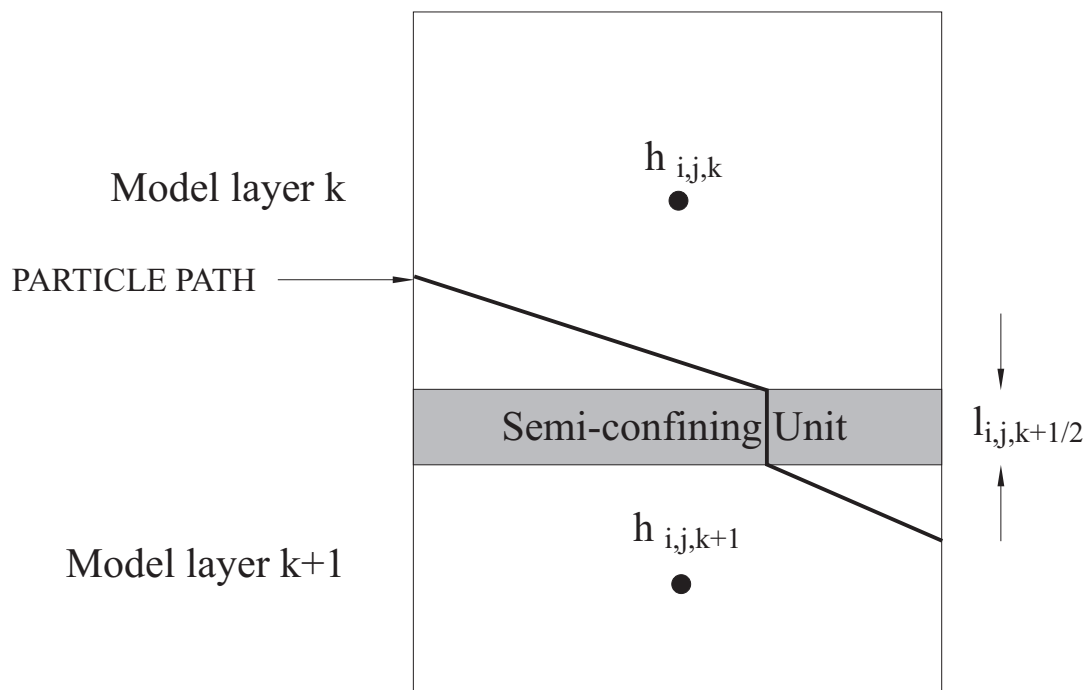
$h_{i,j,k+1}$

Model layer k+1

Figure 3.-- Particle tracking through a semi-confining unit.

For three-dimensional applications, MODFLOW is capable of allowing distorted grids to represent individual geohydrological units that vary in thickness and elevation over the model area. While distortion of the model grid may better represent the flow system, it can also introduce error into the vertical tracking of a particle through the grid if the track does not account for this distortion. An example of distortion is shown in figure 4. The correction implemented in this work is based on the methodology of Pollock (1989, p. 12-14) and Zheng (1994), where particles are tracked from cell face to cell face and the vertical position of a particle is corrected each time the particle moves from one cell to another within a given layer. The correction is calculated such that the ratio of the vertical distance of the particle from the bottom of the cell divided by the vertical length of the cell face is the same for adjoining cell faces.

To demonstrate that the implementation of the particle tracking procedure in ADV is correct, results are compared to published results of MODPATH (Pollock, 1989). The MODPATH sample problem consists of an unconfined aquifer separated from an underlying confined aquifer by a 20-ft thick confining layer (fig. 5). A partially-penetrating well located in the center of the confined aquifer discharges at a rate of 80,000 cubic feet per day. The boundary conditions consist of (1) uniform areal recharge of 0.0045 foot per day to the unconfined aquifer; (2) no flow on all sides and along the bottom of the confined aquifer; and (3) a partially-penetrating river located along one side at the top of the unconfined aquifer. The model grid consists of 27 rows and columns and 5 layers. Grid spacing varies from 40 ft by 40 ft at the well to 400 ft by 400 ft along the model edges. The unconfined aquifer is represented by layer 1 and has a variable thickness of approximately 80 ft. The confined aquifer is represented by four 50-ft thick layers, with the confining layer represented using the quasi-three-dimensional approach.

Many of the features included in MODPATH that populate the model grid with particles are not necessary for the particle tracking included in the ADV package, and it is beyond the scope of this report to reproduce all of the results demonstrated in the MODPATH sample problem. Comparison of the path lines for a cross section taken perpendicular to the river sufficiently demonstrates that the ADV particle tracking duplicates that of MODPATH. The path lines shown in figure 6 were generated using backward tracking from the well located in the cell at row 14 and column 14 of layer 4. The plot shown in figure 6a was generated by MODPATH and is duplicated from Pollock (1989); the plot shown in figure 6b was generated using the ADV package. The circles plotted in figure 6 represent the particle locations in 20-year increments starting from the well; thus, in both cases, the particles are tracked backwards. The two

Uncorrected Position

Corrected Position

Time Step t-1

Layer k

$0.75\ l_{i,j-1,k}$

$0.75\ l_{i,j,k}$

Time Step t

Time Step t+1

Geologic Contact

j-1

j

Column

j+1
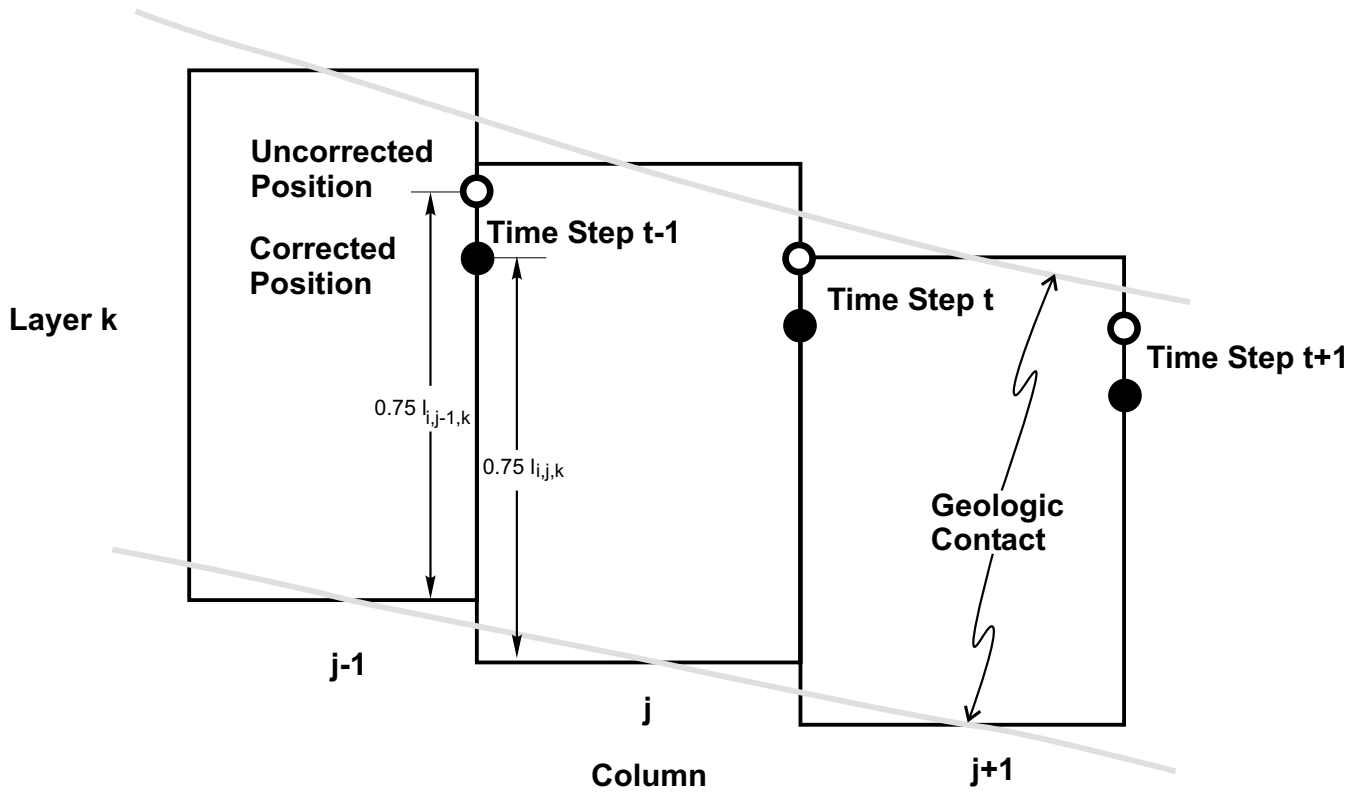
Figure 4.-- Correction to vertical particle position needed for a distorted grid representing a sloping and restricting aquifer (after Zheng, 1994).
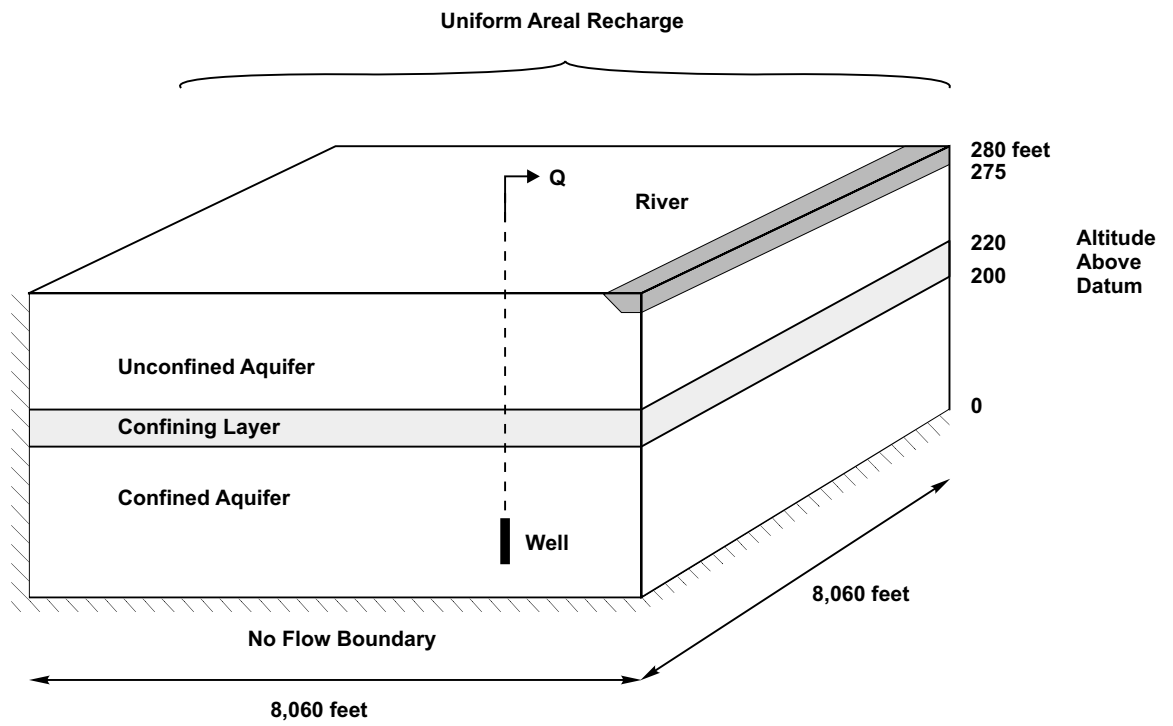
Figure 5.--MODPATH sample problem (after Pollock, 1989).

Column 1

Column 27

(A)

River

ELEVATION, IN FEET

300

200

100

0

Well

HORIZONTAL DISTANCE, IN FEET
Vertical Exaggeration is 5x

0   2,000   4,000   6,000   8,000

(B)

River

ELEVATION, IN FEET

300

200

100

0

Well

HORIZONTAL DISTANCE, IN FEET
Vertical Exaggeration is 5x

0   2,000   4,000   6,000   8,000

Figure 6.--Comparison of MODPATH particle track to ADV particle track. (A) Pathlines presented in Figure 13 of MODPATH documentation (Pollock, 1989); (B) Pathlines obtained using ADV particle-tracking package.

figures are almost identical, indicating that the particle-tracking algorithm included in ADV duplicates MODPATH.

The particle-location sensitivities to the parameters calculated by MODFLOWP using the methodology presented here were tested in a variety of ways during model development. The most critical and easily understood test, however, is whether the calculated sensitivities can be used by the regression to reproduce true parameter values in a synthetic test case. Such an analysis is presented for the synthetic Test Case 1 of the SIMULATION EXAMPLES section.

Estimating Effective Porosity

The ADV Package does not allow effective porosity to be estimated by the regression, which, in some situations, is not expected to be a problem. For example, in Test Case 2 of the section SIMULATION EXAMPLES, the unconsolidated sands have an effective porosity of about 0.39, with little chance of that number being in error by more than 10 percent so that setting the porosity to 0.39 is not likely to cause a problem. In situations where the possible values of effective porosity span a wide range, it will need to be estimated by trial and error using this package. Different values of effective porosity can be assumed and the other parameters can be estimated. Note that head and flow observations provide no information on porosity; such information is available only through the advective-transport observations. Also, evaluation of Darcy's Law shows that advective transport is only sensitive to the ratio of hydraulic conductivity and effective porosity. These characteristics suggest that insensitivity and correlation may be problematic.

Obtaining Advective-Transport Observations

For most applications, it is not clear how to infer observations of the advective-front location directly from concentration data given the complexities contr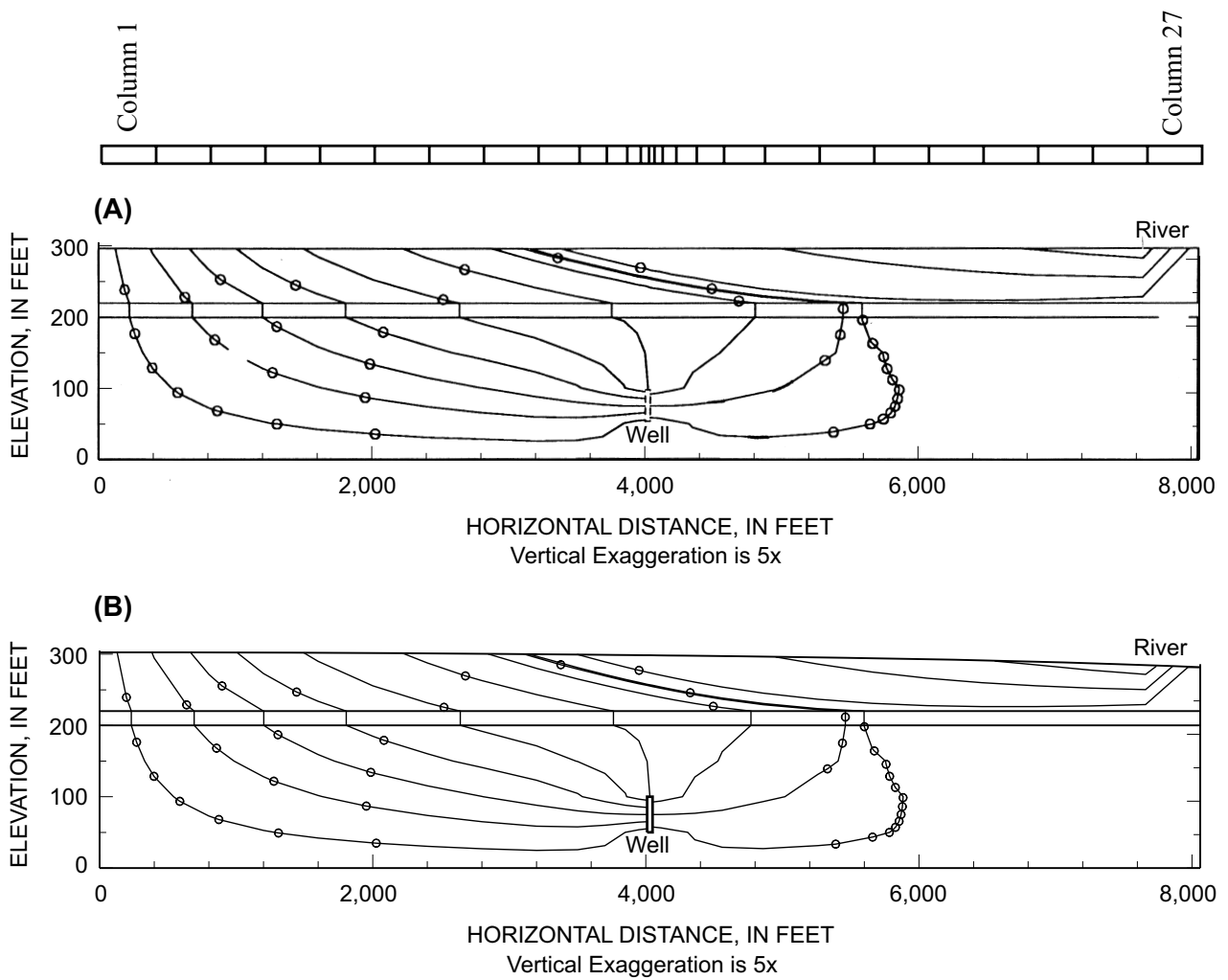ibuting to the transport. Even in the simplest of circumstances, transverse dispersion can cause problems. In addition, in most real world applications, contaminant release history is poorly known, retardation, decay, and chemical reaction are all taking place to some extent, and most flow fields are truly transient. The purpose of this section is to provide some guidance in the selection of an appropriate advective-front location.

A simple analysis can provide some insight into the situation and possibly narrow the range of feasible locations of the advective front. For a continuous source in a one-dimensional flow field with homogeneous hydraulic conductivity in the presence of longitudinal dispersion only, the advective front

is located along the plume centerline at the 50-percent concentration contour (defined as the concentration halfway between the source concentration and the background concentration). In this situation, longitudinal dispersion causes the contaminant front to spread out along the length of the plume, but the advective front is always located at the farthest point from the source on the 50-percent concentration contour (Domenico and Schwartz, 1990, p. 362). By adding the single complexity of transverse dispersion, the plume front stays closer to the source for a given elapsed time of movement than the advective front and the 50-percent concentration contour falls short of the advective front. This problem is illustrated in figure 7, which demonstrates the sensitivity of the location of the 50-percent concentration contour to vertical transverse dispersivity. The presence of transverse dispersion results in the 50-percent concentration contour being located closer to the source than the advective front. The high sensitivity of the location of the 50-percent concentration contour to vertical transverse dispersivity in this problem is due to the small vertical dimension of the contaminant source relative to the horizontal dimension. In general, the location of the 50-percent concentration contour will be more sensitive to situations where transverse dispersion is large in the direction in which the source is small. For example, a tall and narrow source is more sensitive to horizontal transverse dispersion than vertical transverse dispersion, and vice versa.

Analytical solutions can aid in the determination of the advective-front location. An example of this is given by Anderman and others (1996) and Test Case 2 of SIMULATION EXAMPLES, where the two-dimensional strip-source analytical solution of Wexler (1992) was used to determine the range in normalized concentrations at which the plume advective front might occur for a simulation of the sewage-discharge plume at Otis Air Force Base, Cape Cod, Massachusetts. This range was then used with the contoured concentrations to produce a range of uncertainty in the advective-front location. The source size was varied between 600 and 1,200 ft and the transverse dispersivity was varied between 13 and 30 ft, as indicated by LeBlanc (1984a). Results indicated that the normalized concentration of the plume advective front was between 17 and 43 percent.
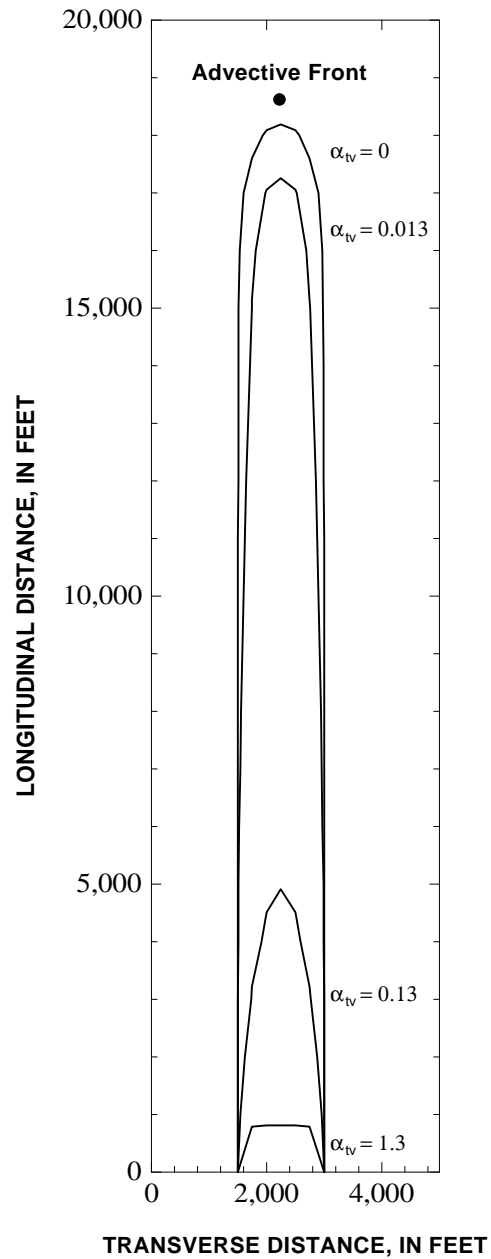
Figure 7.-- Location of the 50-percent concentration contour with varying vertical transverse dispersivity, calculated using Wexler's (1992) three-dimensional strip-source analytical solution.

SIMULATION EXAMPLES

Test Case 1: Example Using Synthetic Data

The validity of the advective-transport observation package calculations was tested using a problem designed to include features relevant to a typical complex three-dimensional MODFLOW model. A synthetic problem was used so that everything is known about the system and parameter values, which allows analysis not possible with field data. The model grid shown in figure 8 has a uniform grid spacing of 1500 m in the horizontal and has 247 active cells in each of three layers. Layers 1, 2, and 3 have a constant thickness of 500 m, 750 m, and 1500 m, respectively. Hydraulic conductivity is divided into four zones, each of which is present in the middle layer and three of which are present in the top and bottom layers (fig. 8). Constant-head boundaries comprise portions of the western and eastern boundaries, with no flow across the remaining boundaries. Head-dependent boundaries representing springs are represented using both the drain and general-head boundary packages. Wells are present at selected nodes, with pumpage at rates ranging from 100 to 200 m^3/d.

Ten parameters were identified for inclusion in the parameter estimation and are described in table 1 along with their true (assigned) values. The observations used in the parameter estimation were generated by running the model with the true parameter values. The locations of the "observed" hydraulic heads are shown in figure 8. The flows simulated at the head-dependent boundaries (fig. 8) were also used as observations in the parameter estimation. Two advective-transport observations were used in the parameter estimation and were generated by injecting one particle each into adjacent cells along the ground-water high and using the final particle locations after a set period of movement. A homogeneous porosity of 0.3 was used.

When exact observations are used (no noise added), the estimated parameter values duplicate the true parameter values to three significant digits (table 1), except for the K2, K3, and K4 parameters. These values, however, are very close to the true parameter values. Based on these results, it can be concluded that parameter estimation using MODFLOWP with the advective-transport package is able to reproduce the true parameter values when exact observations are used in the regression and this forms a test of the sensitivity and regression calculations.
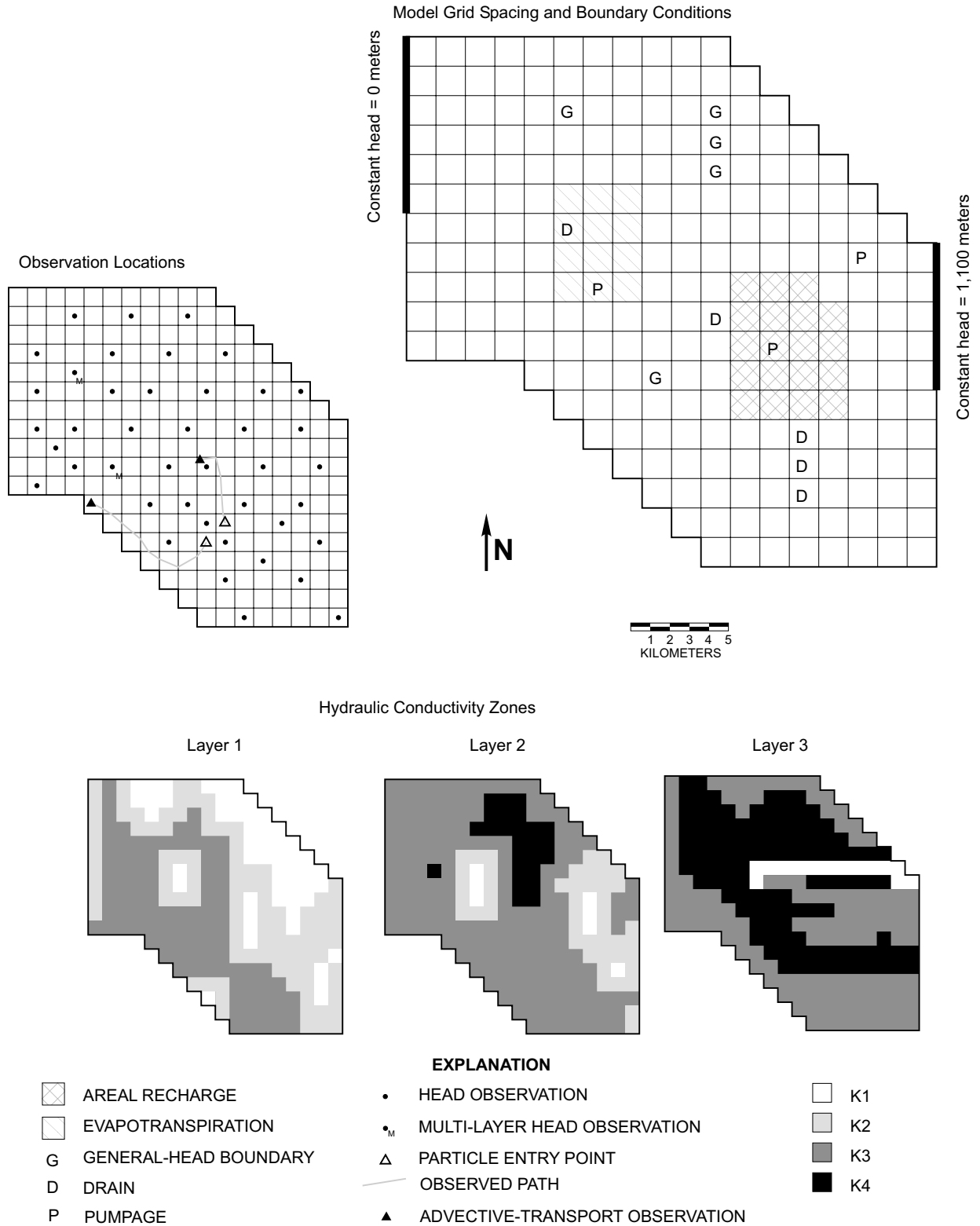
Figure 8.--Test Case 1 model grid, boundary conditions, observation locations and hydraulic conductivity zonation used in parameter estimation.

Table 1. Labels, descriptions and estimated values for the parameters for Test Case 1 [m, meter; d, day].

Label	Description	Units	True Value	Estimated Value
K1	Hydraulic conductivity of zone 1 (see figure 8)	m/d	1.00	1.00
K2	Hydraulic conductivity of zone 2 (see figure 8)	m/d	1.00×10^{-2}	0.99×10^{-2}
K3	Hydraulic conductivity of zone 3 (see figure 8)	m/d	1.00×10^{-4}	0.99×10^{-4}
K4	Hydraulic conductivity of zone 4 (see figure 8)	m/d	1.00×10^{-6}	0.99×10^{-6}
ANIV1	Vertical anisotropy of layers 1 and 2		4.00	4.00
ANIV2	Vertical anisotropy of layer 3		1.00	1.00
RCH	Areal recharge rate applied to the area shown in figure 8	m/d	3.10×10^{-4}	3.10×10^{-4}
ETM	Maximum evapotranspiration rate applied to area shown in figure 8	m/d	4.00×10^{-4}	4.00×10^{-4}
GHB	Conductance of head-dependent boundaries G shown in figure 8 represented using the general-head boundary package.	m^2/d	1.00	1.00
KDR	Conductance of the head-dependent boundaries D shown in figure 8 using the drain package.	m^2/d	1.00	1.00

Test Case 2: Example Using Field Data

The ADV Package was applied to the sewage-discharge plume at Otis Air Force Base on the Massachusetts Military Reservation in Cape Cod, Massachusetts (fig. 9) to demonstrate, using a previously published field-site simulation, the use of advective-transport observations in model calibration with parameter estimation accomplished using nonlinear regression. The site was chosen because field studies had been conducted to characterize the plume and hydrogeological setting of the area, and a two-dimensional ground-water flow model had been developed using trial-and-error calibration by LeBlanc (1984a). This test case is presented by Anderman and others (1996), but is repeated here to provide insight into the use of advective-transport observations in ground-water flow model calibration. In addition, the test case illustrates some useful procedures that are applicable regardless of the types of observations considered.

Site Description

The regional aquifer is part of an outwash plain and consists of an approximately 330-ft thick unit of unconsolidated sediment overlying relatively impermeable bedrock (LeBlanc and others, 1991). The aquifer consists of 100 ft of unconsolidated sand and gravel sediments, which are underlain by an aquitard consisting of approximately 230 ft of fine-grained sand and silt. Regional estimates of hydraulic conductivity of the aquifer based on grain-size distributions, ground-water flow model calibration, and one aquifer test range from 140 to 370 ft/d (LeBlanc, 1984a; LeBlanc and others, 1991). Flow-meter analyses on 16 long-screened wells in a gravel pit adjacent to Ashumet Pond yielded an average hydraulic conductivity of 310 ft/d (Hess and others, 1992). The effective porosity of the outwash determined from spatial moments analysis of several small-scale tracer tests is about 0.39; vertical
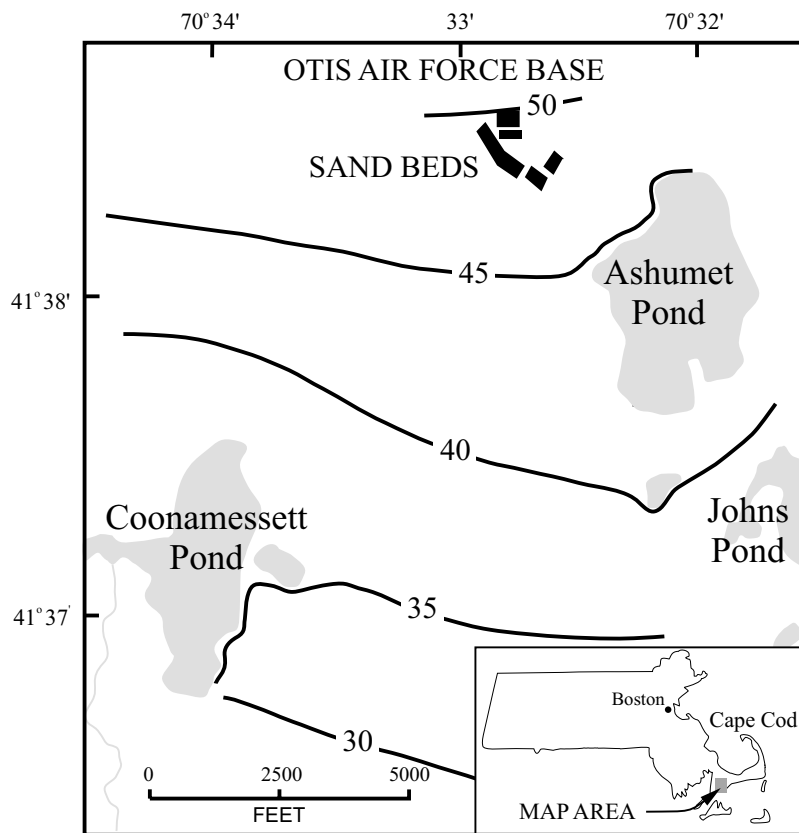
23

Figure 9.-- Location of Otis Air Force Base, water-table elevation contours, and sewage-discharge sand beds for Test Case 2 (after LeBlanc, 1984b).

24

gradients within the aquifer are small and ground-water flow in the aquifer can be considered to be horizontal, with an average regional flow to the south-southwest (LeBlanc and others, 1991).

The plume emanates from sand beds (fig. 9) used for sewage disposal since the 1930's, although appreciable discharge to the beds did not commence until the early 1940's. A number of physical properties and chemical constituents have been monitored to determine the extent and migration of the sewage plume. Boron, contoured by LeBlanc (1984a) during 1978-79 measurements (fig. 10), is a good indicator of plume movement because of its high concentration relative to uncontaminated groundwater. Data suggest that boron transport is slightly retarded (Warren Wood, U.S. Geological Survey, written commun., 1994), but analysis of the retardation rates indicated that the effect on inferred rates of advective transport are negligible.

Ground-Water Flow and Parameter-Estimation Models

The movement of contaminants in the sewage-discharge plume was simulated using a two-dimensional finite-difference ground-water flow model based on the model developed by LeBlanc (1984a) (fig. 10A). The model has 34 500-ft wide columns and 38 750-ft long rows, with 957 active cells. LeBlanc (1984a) used a homogeneous hydraulic conductivity of 186 ft/d; recharge to the aquifer from precipitation of 19.8 in/yr, with no recharge over Ashumet Pond; specified flux across the northern boundary at about the 60-ft water-table contour of 2.3 ft^3/s; constant head along (1) the southern boundary at about the 10-ft water-table contour, (2) Coonamessett Pond and River on the west side of the model and (3) Johns Pond and the Childs River on the east side. Ashumet Pond was represented as a general-head boundary, with two zones of conductance: the outer shoreline zone had ten times the hydraulic conductivity and one-fifth the thickness of the inner zone. The decrease in aquifer thickness beneath the pond was simulated by tapering the saturated thickness of the layer beneath the pond to one-half of the saturated thickness of the aquifer. There were two head-dependent river reaches simulated within the model area: Cranberry Bogs near the southern boundary of the model, and the area north of Johns Pond on the eastern boundary of the model. The sewage-discharge sand beds were represented as a specified-flux boundary with a flux of 0.72 ft^3/s, which is based on estimates of historical discharge. The boundaries north of Coonamessett and Johns Ponds correspond to ground-water flow lines and are simulated as no-flow boundaries.

Five parameters were identified for estimation by the parameter-estimation model: (1) the homogeneous hydraulic conductivity (K), (2) areal recharge (RCH), (3) flux at the northern boundary (Qn), (4) flux at the sewage-discharge beds (Qb), and (5) the conductance of the low hydraulic

25

(A)

COLUMNS OF MODEL GRID

(B)

Sewage Discharge Sand Beds

Particle Entry Point

Ashumet Pond

1,000 2,000 3,000
SCALE IN FEET
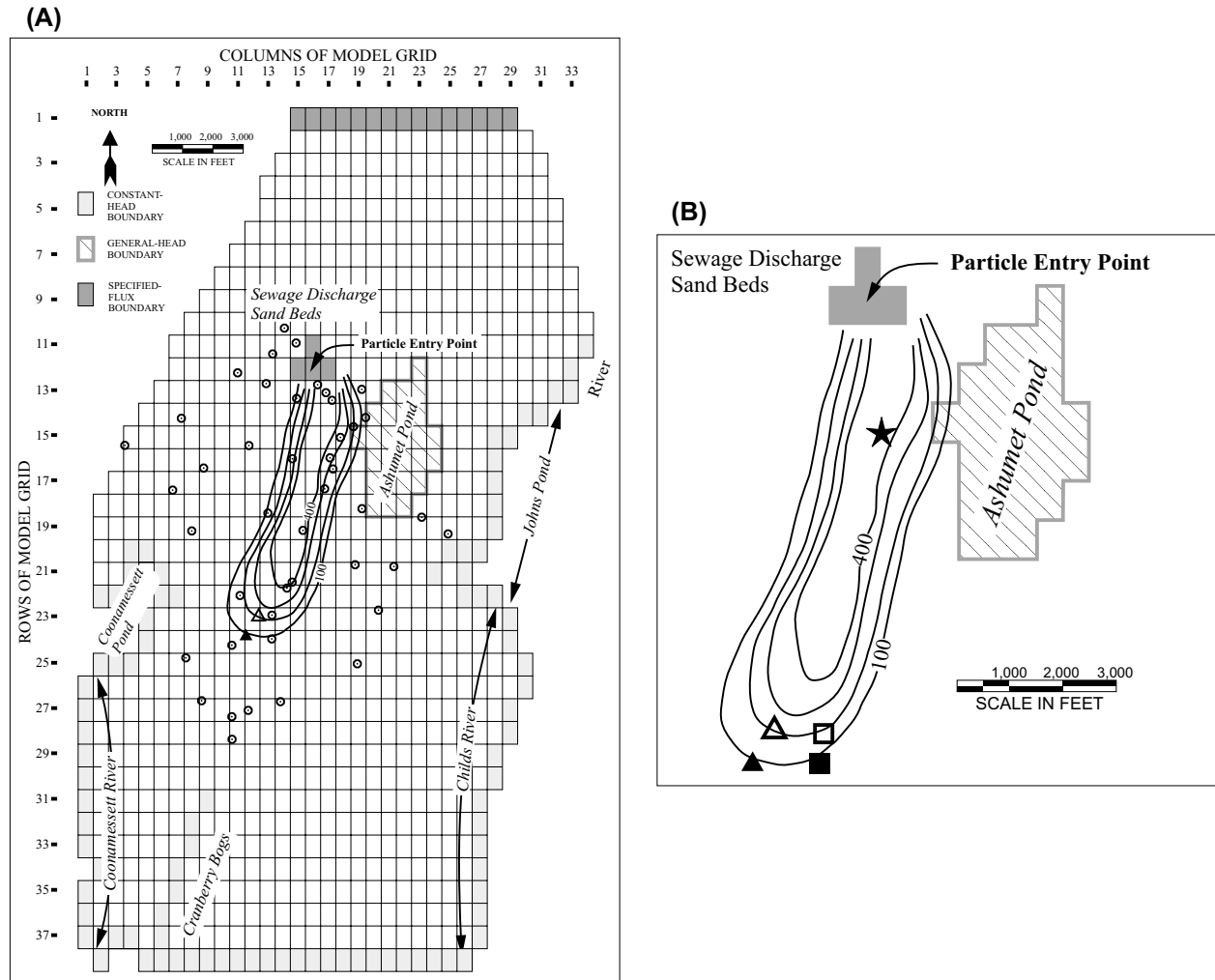
EXPLANATION

◉   WATER-LEVEL OBSERVATION WELL -- Site where water levels were observed in November 1979.

——100——   LINE OF EQUAL BORON CONCENTRATION, 1978-79 -- Interval 100 micrograms per liter.

▲ △   PLUME-FRONT OBSERVATION -- Locations of advective plume front determined using an analytical solution and extremes in transverse dispersion and source size values, respectively.

★   PREDICTED PLUME-FRONT LOCATION -- Final particle position calculated using parameter values estimated only with head and flow observations.

■ □   PREDICTED PLUME-FRONT LOCATION -- Final particle positions calculated using parameter values estimated with head and the extremes of the advective-transport observations, respectively.

Figure 10.-- (A) Test Case 2 finite-difference grid, water-level observation wells, boron concentrations of contaminated ground water, and advective-transport observation locations used in the regression (after LeBlanc, 1984a); (B) Detail of the sewage-discharge plume and advective-front locations calculated using the sets of estimated parameter values shown in tables 3B, 3C and 3E.

conductivity zone of Ashumet Pond (GHB) (the conductance of the outer zone equals this parameter value times 50). The inclusion of specified-flux boundary conditions as parameters allowed their values to vary with changes in the hydraulic-conductivity parameter, as would be expected. Inclusion of a sixth parameter representing the conductance of Coonamessett and Childs Rivers caused unstable regression results due to its insensitivity; thus, the rivers are represented using constant-head cells for the results presented. The ground-water flow model developed for the present work duplicates that described by LeBlanc (1984a) when his parameter values are used.

Observations used in the parameter estimation included: (1) 44 measured hydraulic heads, which are considered to be accurate, (2) a head-dependent boundary recharge of 0.4 ft^3/s from Ashumet Pond determined from a water budget, which is considered to be somewhat unreliable, and (3) observed x- and y-locations of the advective front estimated from the boron concentration contours, which are considered to be somewhat reliable. The locations of Ashumet Pond, the water-level observation wells, and the advective-transport observations are shown in figure 10A. The triangles on figure 10 represent the extreme advective-front locations estimated based on the analysis procedure described in the section OBTAINING ADVECTIVE-TRANSPORT OBSERVATIONS. Use of the two observations allowed for investigation of how uncertainty in advective-front observations affect parameter-estimation model results. To simulate the advective transport, a single particle was introduced into the ground-water system at the approximate center of the plume source in the middle of the cell in row 12, column 16 (fig. 10a), and was allowed to move for the 38-year period between appreciable discharge to the aquifer and the time of observation.

The weights of these observations were calculated using the following statistics, as discussed after Equation (1): The standard deviation of the 44 accurate hydraulic-head measurement errors was assumed to be 0.1 ft; the coefficient of variation (standard deviation divided by the measured value) of the somewhat unreliable head-dependent boundary error was assumed to be 0.5; the standard deviation of each of the somewhat reliable advective-front movement observations was assumed to be 500 ft (the width of a grid cell) in both the x- and y-directions.

Analysis Procedure

To quantify the effect of observation type, the parameter-estimation model was run with six different sets of observations: (1) head observations alone, (2) head and flow observations, (3, 4) head and each of the two advective-transport observations, and (5, 6) head, flow and each of the two advective-transport observations.

Each data set was evaluated in two ways, which are presented here because of their utility in inverse modeling. First, in a preliminary analysis, initial parameter value regression statistics, including the overall parameter sensitivities and correlations, were calculated at the parameter values reported by LeBlanc (1984a). Correlations are obtained at initial parameter values by forcing the parameter estimation to converge at the initial values (that is, by setting the maximum parameter change with each iteration and the parameter closure tolerance criterion [DMAX and TOL of MODFLOWP; Hill, 1992, p. 148] equal to 1×10^{-3} and 1×10^9, respectively). Results from the preliminary analysis can be used to identify parameter insensitivity and correlation that is likely to cause problems in the nonlinear regression and to evaluate the likely effect of any new or proposed observation on parameter sensitivity and correlation. This information can then help guide redefinition of the parameters, if necessary. Because the ground-water flow equation is nonlinear with respect to many estimated parameters, the results indicated at the initial parameter values may differ from the results calculated at other sets of parameter values, but the major characteristics are often similar. In a second set of model runs, parameter values are optimized using nonlinear regression, and their overall sensitivities, correlations, and coefficients of variation are calculated. The statistics used in the analysis are discussed more fully in the following paragraphs.

The overall sensitivity of the observations to the parameters reflect how well the parameters are defined by the observations and indicate how well the parameters will be estimated. Composite scaled sensitivities are used to measure this overall sensitivity and are calculated by MODFLOWP as follows. First, the sensitivities are scaled by multiplying them by the product of the parameter value and the square root of the weight of the observation to obtain dimensionless values. The scaled sensitivities for each parameter are then squared and the sum of these values is divided by the number of observations. The composite scaled sensitivities equal the square root of these values and are taken from the MODFLOWP output at the end of the table labeled SCALED SENSITIVITIES, which is printed when ISCALS equals 1 on line 6 of the Parameter Estimation input file (Hill, 1992, p. 133). The scaling depends on the parameter values, and, for nonlinear parameter-estimation models, the sensitivities depend on the parameter values. Consequently, the composite scaled sensitivities will be different for different parameter values. As mentioned above, however, the major characteristics are often similar. The authors' experience indicates that if the composite scaled sensitivity values for each of the parameters vary by more than two orders of magnitude from each other, the optimization procedure often has difficulty estimating values for the less sensitive parameters.

Correlation between parameters indicates whether or not the parameter estimates are unique with the given model construction and observations, depending on how well the parameters are defined by the observations, as previously discussed. Correlations range between -1 and 1, with absolute values close to 1 indicating a high degree of correlation. If two parameters are highly correlated, then changing the parameter values in a linearly coordinated way will result in a similar value of the objective function. Parameter correlation is a concern in trial-and-error calibration as well, but may be unknown to the modeler; the use of regression makes parameter correlation obvious. Although there is debate over what correlation values are significant, the authors' experience has indicated that there is enough information in the observation data so that parameters can be uniquely estimated if their correlation is less than 0.98. For correlations with absolute values larger than 0.98, uniqueness of the solution can be evaluated by starting parameter estimation at different initial values. If all runs produce nearly the same estimates, the solution is probably unique.

The coefficients of variation of the estimated parameter values are calculated as the standard deviations of the parameter estimates divided by the estimated parameter values. Values much less than 1.0 occur when the parameter has a large overall sensitivity and indicate a precise parameter estimate.

Results

At the LeBlanc parameter values (table 2), composite scaled sensitivities are not significantly affected by either the flow or transport observation, but the flow observation (table 2B) reduces the correlations more than the advective-transport observation (table 2C).   The complete parameter correlations produced when head observations (table 2A) are used alone indicates it will be impossible to estimate parameters independently with head observations alone. Adding flow or advective-transport observations reduced some of the correlations, but the remaining correlations of 1.0 and the low sensitivity for the Ashumet Pond (GHB) conductance still indicate possible problems. These results suggest that, as weighted: (1) the flow observation is more valuable to the regression than the advective-transport observations, (2) both additional observations can help to reduce the extreme correlation that occurs when only hydraulic-head observations are used to estimate parameter values, and (3) problems with the regression are likely. Further investigation showed that at the initial parameter values the advective-transport observation does not significantly reduce the correlations because the particle only travels a short distance and discharges into Ashumet pond. This may indicate that, in this case, the analysis procedure is limited because the starting parameter values produce unreasonable advective

Table 2.--Parameter sensitivities and correlations calculated for the initial parameter
for Test Case 2

[The labels K, RCH, Qn, Qb, and GHB are used to identify the following estimated
parameters: K, hydraulic conductivity; RCH, recharge rate; Qn, northern boundary
flux; Qb, sewage-discharge sand bed flux; GHB, Ashumet Pond conductance.]

	K	RCH	Qn	Qb	GHB
LeBlanc's Values	186	19.8	2.3	0.72	64,800

A. Head observations only					
Composite sensitivity	39.0	29.9	6.57	3.88	0.0572
Correlation calculated at initial values					
RCH	1.00				
Qn	1.00	1.00			
Qb	1.00	1.00	1.00		
GHB	1.00	1.00	1.00	1.00	

B. Head and flow observations					
Composite sensitivity	39.0	29.8	6.57	3.86	0.0568
Correlation calculated at initial values					
RCH	1.00				
Qn	0.93	0.92			
Qb	0.72	0.71	0.43		
GHB	0.01	0.00	-0.01	0.26	

C. Head and near advective-transport observations					
Composite sensitivity	38.2	29.2	6.43	3.80	0.0571
Correlation calculated at initial values					
RCH	1.00				
Qn	1.00	1.00			
Qb	1.00	1.00	1.00		
GHB	0.75	0.75	0.75	0.76	

transport. It also indicates the importance of investigating the model fit associated with the initial parameter values.

The model fits achieved in the regression presented in table 3 are summarized as follows. Table 3A shows that regression was not possible using head data alone. The addition of the flow observation reduced the correlation so that the regression converged, which is consistent with the preliminary analysis, but the optimal parameter values shown in table 3B are unreasonably small. At the optimal parameter values produced using the advective-transport observations (tables 3C and 3E), the parameters are less correlated than at the optimal parameter values produced using the flow observation (table 3B), which is inconsistent with the preliminary analysis above. Inspection of the results indicated that this inconsistency was caused by the fact that, with LeBlanc's values, the particle exited into Ashumet Pond, as noted above. The smaller coefficients of variation produced using the advective-transport observations indicate the estimates are more precise than those produced using the flow observation. Using all the observations (tables 3D and 3F) results in parameter estimates, correlations, and coefficients of variation that are very close to those using the head and advective-transport observations. The small composite scaled sensitivity and large coefficient of variation for the northern boundary flux and Ashumet Pond conductance indicate that these parameters are not well defined with the available observations and given model construction.

When parameter values were optimized using nonlinear regression, the total objective function (S of Equation 1) was reduced from about 4,500 to about 1,700 for all simulations. This results in a calculated error variance of 39, suggesting that the model fit to the data is worse than would be consistent with the subjectively determined standard deviations and coefficient of variation by, on average, a factor of the square root of 39, or about 6. This difference could be due to neglecting some components of the measurement error or to neglecting model error. The traditional approach (Carrera and Neuman, 1986a; Cooley and Naff, 1990) is to alter the weighting to achieve a match between the common and calculated error variances; this approach is confusing, however, when many types of observations are used in the regression.

The reduction of the objective function for all regression runs, which started at the Leblanc values, were similar as follows: for hydraulic heads, S_h decreased from about 4,150 to about 1,675, and unweighted hydraulic-head residuals only exceeded 1.0 ft at five observation points and did not exceed 1.5 ft (3 percent of the total 50 ft head drop across the system and substantially larger than the 0.1 ft standard deviation used to weight the head observations); for the flow out of Ashumet Pond, S_f increased from 5 to about 20, and the unweighted residual did not exceed 0.86 ft^3/s (215 percent of the observed

Table 3.--Optimal parameter estimates, parameter sensitivities, and correlations for Test Case 2

[The labels K, RCH, Qn, Qb, and GHB are used to identify the following estimated parameters: K, hydraulic conductivity; RCH, recharge rate; Qn, northern boundary flux; Qb, sewage-discharge sand bed flux; GHB, Ashumet Pond conductance. Values in parentheses are the total number of parameter-estimation iterations required to satisfy a convergence criteria of 0.01; * indicates convergence was not achieved in 15 iterations, estimates from the final iteration are reported; - -, not calculated because parameter estimation did not converge.]

	K	RCH	Qn	Qb	GHB
LeBlanc's / Initial Values	186	19.8	2.3	0.72	64,800

	A. Head observations only (*)					B. Head and flow observations (8)				
	K	RCH	Qn	Qb	GHB	K	RCH	Qn	Qb	GHB
Estimated value	209	14.5	4.1	0.80	1,490	46	3.2	0.9	0.18	328
Composite sensitivity	35.2	21.2	11.5	4.21	1.25	34.9	21.0	11.4	4.19	1.22
Coefficient of variation	- -	- -	- -	- -	- -	3.4	3.4	3.5	3.6	3.6
	Correlation calculated at optimal values					Correlation calculated at optimal values				
RCH	1.0					1.00				
Qn	1.0	1.0				0.99	0.99			
Qb	1.0	1.0	1.0			0.94	0.94	0.89		
GHB	1.0	1.0	1.0	1.0		0.96	0.95	0.95	0.92	

With Near Boron Plume Observation										
	C. Head and advective-transport observations (6)					D. All observations (6)				
	K	RCH	Qn	Qb	GHB	K	RCH	Qn	Qb	GHB
Estimated value	158	10.9	3.1	0.60	1,122	147	10.2	3.0	0.49	955
Composite sensitivity	34.5	20.7	11.4	4.06	1.22	34.5	20.7	11.7	3.58	1.27
Coefficient of variation	0.3	0.3	0.6	1.3	1.1	0.3	0.4	0.6	1.4	1.0
	Correlation calculated at optimal values					Correlation calculated at optimal values				
RCH	0.95					0.96				
Qn	0.63	0.55				0.68	0.60			
Qb	0.14	0.08	-0.59			0.07	0.02	-0.60		
GHB	0.31	0.17	0.24	0.26		0.31	0.17	0.27	0.23	

With Distant Boron Plume Observation										
	E. Head and advective-transport observations (6)					F. All observations (6)				
	K	RCH	Qn	Qb	GHB	K	RCH	Qn	Qb	GHB
Estimated value	169	11.7	3.3	0.63	1,200	158	11.0	3.2	0.51	1,009
Composite sensitivity	34.5	20.7	11.4	4.04	1.20	34.7	20.8	11.9	3.48	1.29
Coefficient of variation	0.3	0.3	0.6	1.3	1.1	0.3	0.3	0.6	1.4	1.0
	Correlation calculated at optimal values					Correlation calculated at optimal values				
RCH	0.94					0.95				
Qn	0.60	0.50				0.66	0.56			
Qb	0.10	0.03	-0.65			0.04	-0.02	-0.64		
GHB	0.28	0.12	0.21	0.25		0.28	0.13	0.25	0.21	

flow or about 4 times the coefficient of variation used to weight the flow observation); for the near advective-transport observation, S_t decreased from 173 to less than 5, and the x- and y-residuals did not exceed 1,050 and 560 ft, respectively (roughly double and equal to the standard deviations, respectively, used to weight the advective-transport observations); for the distant advective-transport observation, S_t decreased from 218 to less than 10, and the x- and y-residuals did not exceed 1,360 and 565 ft, respectively (roughly two and a half times and equal to the standard deviations, respectively, used to weight the advective-transport observations).

These results indicate that the lack of model fit that resulted in the error variance of 39 was spread throughout the observations, and that no one type of observations was fit better overall than another, as is required for a valid regression. Analysis not included in this report indicates that the weighted residuals are independent and normally distributed. There is an area of the model west of Ashumet Pond and north of Coonamessett Pond, however, where the calculated heads are consistently higher than the observed heads, suggesting there is some bias in the model. The source of this bias was not determined in this study.

The parameter values estimated when the distant advective-transport observation is used (tables 3E and 3F) are an average of seven percent higher than those estimated when the near observation is used (tables 3C and 3D). This can be explained by the difference in the observed locations (fig. 10): the distant observation implies that the advective front is moving with an average velocity of 0.65 ft/d, eight percent faster than the average velocity of 0.60 ft/d implied by the near observation. Ninety-five percent linear individual confidence intervals calculated for the two sets of parameter estimates largely overlap, indicating that the estimated values are not statistically different. Thus, for this model, even though the location of the advective-front is not well known, the parameter estimates do not change significantly given reasonable uncertainty in the advective-transport observation.

Discussion

Advective-transport observations reflect ground-water velocities and patterns over a long period of time and provide more complete information about the ground-water flow system than flow measurements taken at a discrete point in time. This results in different estimated parameter values when different observation types are used (tables 3B, 3C, and 3E) and has a significant impact on the probable accuracy of the transport predictions of the model. Figure 10B shows that the advective-front location simulated using the parameter values estimated with only the head and flow observations (represented by the star) is at least 6,085 feet from the plume-front observation locations (represented by the open and

33

closed triangles), while the locations simulated using the parameter values estimated with only the head and advective-transport observations (represented by the open and closed squares) are at most 1,275 feet from the plume-front observation locations. This illustrates that the use of advective-transport observations in the parameter estimation results in a model that more accurately represents the movement of the sewage-discharge plume than use of the flow observation. Results not presented in this report also show that the particle-position sensitivities and flow sensitivities are of opposite sign, which means that the particle-position and flow observations influence the parameter values to change in opposite directions.

It is interesting to note that in simulations in which only one observation reduces correlation in an otherwise completely correlated set of parameters, the simulated equivalent to that observation is always very close to the observed value. In Test Case 2, this occurs in simulations with only the flow observation or only the advective-transport observations. In this circumstance, the close match does not necessarily indicate an accurate simulation, but is an artifact of the relation between the data and the parameter values, and any error in that observation is directly translated into the solution. In many cases confidence intervals will be large, reflecting the underlying uncertainty.

Ground-water flow model validity can be judged by evaluation of the reasonableness of the parameter estimates and the lack of bias in the weighted residuals (Draper and Smith, 1981; Cooley and Naff, 1990). For all simulations using the advective-transport observations, the estimated values of horizontal hydraulic conductivity (K) are within the reported range of 140 to 370 ft/d and, with a coefficient of variation of about 0.3 (table 3), can be considered to be precisely estimated with the available data. The estimated northern boundary flux (Qn) is roughly 1.3 times the flux used by LeBlanc (1984a), which is not unreasonable considering how little is known about this flux. The estimated sewage discharge flux (Qb) is roughly two-thirds of LeBlanc's value, which may be a little low, but is reasonable considering precise estimation was not possible with the available data, as indicated by the large coefficient of variation of 1.3 to 3.6.

The estimated Ashumet Pond conductance (GHB) and recharge (RCH) parameter values for the simulation using all observations (tables 3D and 3F) are about a factor of 64 and 2, respectively, less than the values used by LeBlanc (1984a). It is difficult to evaluate whether the estimated Ashumet Pond conductance parameter value is reasonable given the lack of field data. Considerable independent information, however, indicates that the recharge rate should be close to 20 in/yr (LeBlanc, 1984a), so the estimated 11 in/yr recharge rate appears to be unreasonably small. Possible explanations developed as part of this study include: (1) the heads used in the model were observed in November and may not

represent average annual conditions, and (2) the elevations of the constant-head boundaries were determined from 10-ft contour topographic maps, and, therefore, are subject to errors of 5 ft or more. The seasonal variation in the water-table elevation is 1 to 3 feet, with the lowest heads occurring in late fall (LeBlanc, 1984b). The importance of the observation and boundary-head elevations to the model was investigated by estimating parameter values with all the observations with the distant advective-transport observation and (1) all the observed-head elevations increased by 1 ft, or (2) all the constant-head elevations decreased by 1 ft. Increasing all the observed head elevations resulted in an estimated recharge rate of 22.1 in/yr, while decreasing the constant-head elevations resulted in an estimated recharge rate of 15.2 in/yr. These results suggest that model results are sensitive to the relationship between the observed heads and the constant-head boundary heads, and, therefore, that it is important to measure all head elevations used in the model at the same time. These results also demonstrate how nonlinear regression can be used to test different aspects of model calibration.

FIRST-ORDER UNCERTAINTY ANALYSIS

Output from the ADV package is compatible with the five post-processors for testing residuals and calculating linear confidence and prediction intervals from MODFLOWP results (Hill, 1994). Specification of unit numbers IOUYR and IUNORM on line 7 of the MODFLOWP input file (Hill, 1992, as augmented by the readme.doc distributed with MODFLOWP) produces output files equivalent to the programs YR and NORM (Hill, 1994) and replace these programs. Specification of unit numbers IOUE on line 7 and IOUR in data set 13B produce input files that can be used by the programs BEALEP, RESANP, and YCINT (Hill, 1994). As documented by Hill (1994), the user must manually produce the input file to be used in the BCINT program from parts of the MODFLOWP output file.

The confidence intervals calculated by YCINT for calibrated or predicted conditions can be used to construct confidence interval regions for the predicted advective-transport observations. Output from YCINT consists of confidence intervals along the x-, y-, and z-coordinate directions. It can be useful to simply plot these confidence intervals on their respective axes, as shown in a plot of the x-y plane for Test Case 1 (fig. 11A). Alternatively, in some situations, the limits of the confidence intervals can be thought of as points on an ellipse, which can then be plotted to represent confidence regions. The limits of such a region indicate the probable area in which the predicted advective-transport location could result. The confidence interval limits do not, however, by themselves define an ellipse. One possible
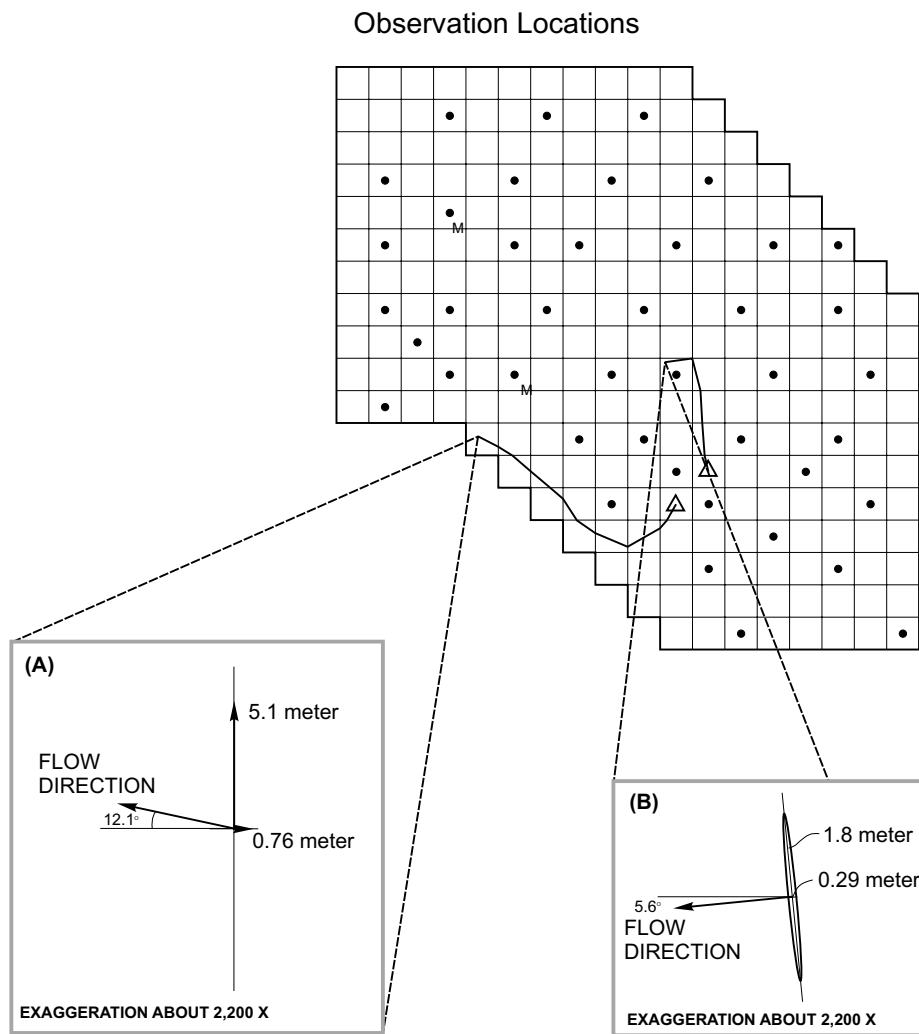
35

Observation Locations

Figure 11.--95-percent confidence ellipses for final calibrated advective-transport observations for Test Case 1. (A) Intervals plotted on their respective axes; (B) Intervals plotted as an ellipse.

way to define an ellipse is to require that one of its axes be aligned with the direction of flow. An example of an ellipse constructed in this way is shown in figure 11B.

Because noiseless observations were used in the parameter estimation, the confidence intervals shown in figure 11b are smaller than would be encountered for most models. The scale of the ellipses is much smaller than the scale of the model so that the ellipses are exaggerated roughly 2,200 times in figure 11. It is interesting to note, however, that for both calculated particle locations the confidence interval parallel to the flow direction is much smaller that the interval perpendicular to the flow direction. This is consistent with larger scaled sensitivities in the y-direction relative to the x-direction.

COMMON PROBLEMS

A number of problems are commonly encountered when using advective-transport observations in regression. Some of the most common are discussed here. Note that use of advective-transport observations may not be appropriate for all situations.

1. Problem: The particle track at the initial parameter values is very different than the observed track.

   Discussion: Commonly a particle will track in a very different direction than observed using the initial parameter values and perhaps exit the model grid prematurely. For example, the particle track at the initial parameter values for the Otis Air Force Base model of Test Case 2 exits into Ashumet Pond, as shown in figure 12. This results in large advective-transport residuals, and smaller than expected sensitivities that are not reflective of the true worth of the data.

   Resolution: Often this problem resolves itself. As the parameter values are changed by the regression during the parameter estimation iterations, so that they are more reflective of the actual system, generally the simulated particle track will also start looking more like the observed track. For example, the final particle position for Test Case 2 is very close to the observed plume-front location (fig. 10b). If it does not resolve itself and the final track is incorrect, see Problem 2.

2. Problem: The particle track at converged parameter values is much different than the observed track.
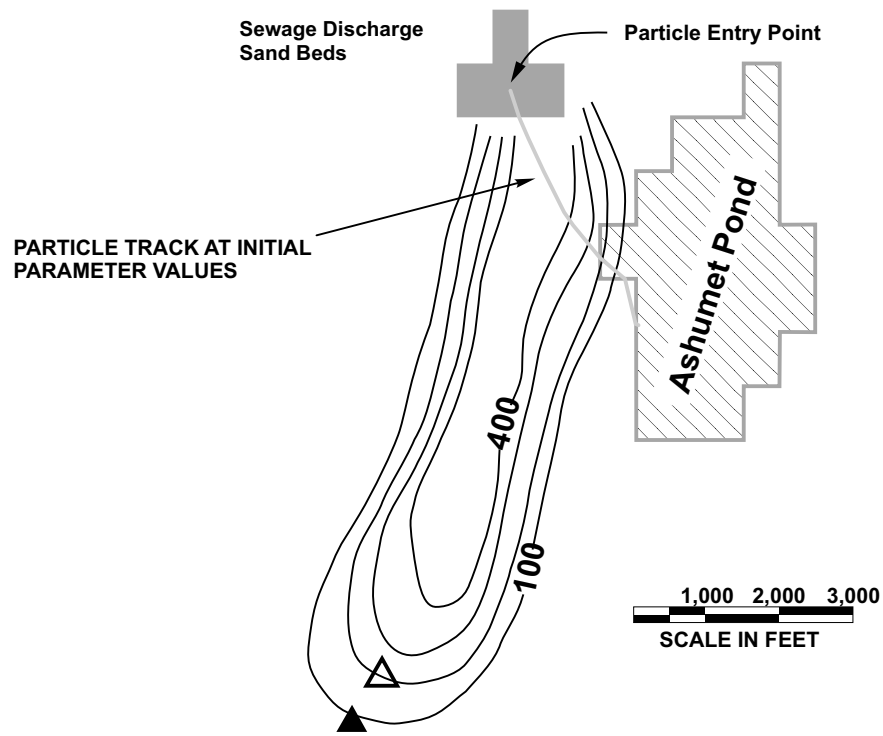
Figure 12.-- Example of unrealistic particle track at initial parameter values for Test Case 2.

Discussion: Possible causes include: (a) the entry point of the particle into the system is incorrect, (b) one of the other observations or prior information may be dominating the regression, and (c) there are errors in the conceptual representation of the system.

Resolution: For (a), it is important that the point where the particle is introduced into the model grid be chosen with care. If the entry point is located on a high point in the water table from which flow diverges, then this point may move around with differing parameter values and the resulting particle track can be very erratic. Likewise, if the entry point is close to a dominant ground-water sink, the particle may track towards the sink and exit the system prematurely. Changing the entry point even slightly may result in a more realistic particle track and it may take a few trial runs to obtain an entry point that seems appropriate. If, however, a problem is very sensitive to different, but equally likely, initial particle placements, this should be discussed in any description of the calibration effort. For (b), it is recommended that the data from which the observations and their weights were calculated be carefully scrutinized. Observations that have large weighted residuals and scaled sensitivities will dominate the regression and should be looked at first. Specifically, look at how the water-table elevations were determined, and whether well-head elevations were surveyed precisely or taken from a topographic map. Alternatively, if the model grid-cell spacing is large and the water table has a steep gradient, model error may be a larger factor than anticipated. An observation that is causing a problem may be either less precise than initially indicated, so that the statistic from which the weight is calculated should be increased, or it may be inaccurate, so that it should be omitted from the parameter estimation. For (c), any of the assumptions on which the conceptual model is based may be in error. Commonly, aquifer heterogeneity is oversimplified or incorrectly specified, or specified boundary conditions are in error. Again, scrutinize the model setup and correct any mistakes.

3. Problem: Complex particle tracks may cause the regression not to converge.

Discussion: An example of this problem occurred for Test Case 1 (fig. 13). Here, the particle is introduced into the system at the water table (layer 1) in row 12 and column 13, travels to layer 2, back up to layer 1, descends to layer 3, traverses the model, and finally emerges from layer 1 with evapotranspiration in row 7 and column 7. This circuitous path follows patches of high hydraulic conductivity. When the coordinates of the endpoint of this path are included as observations, the parameter estimation oscillates
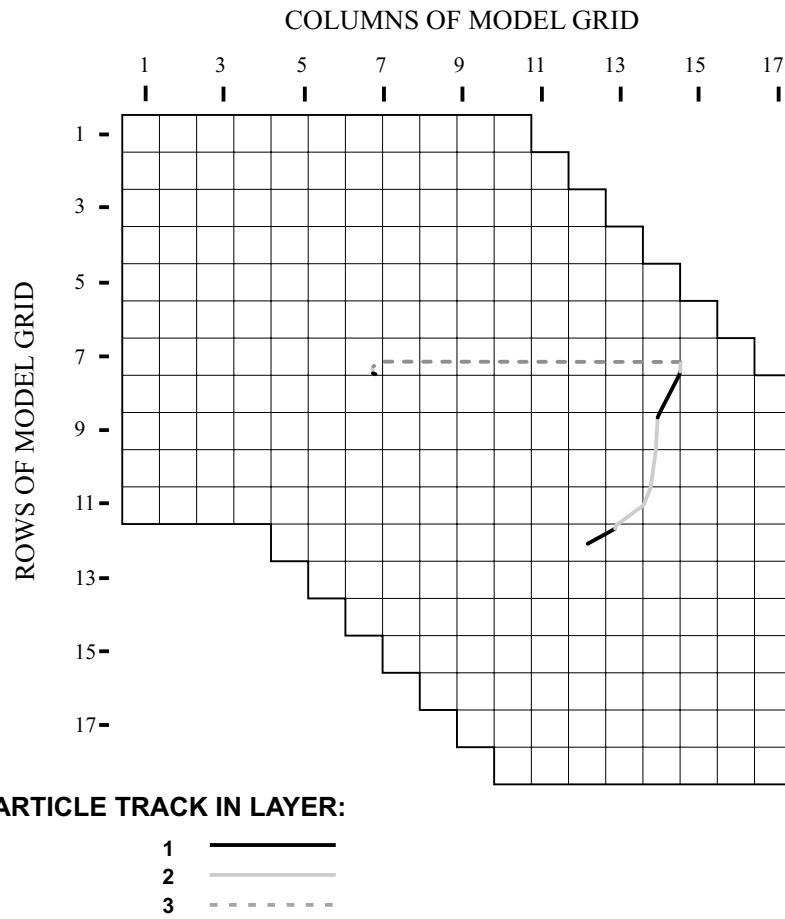
COLUMNS OF MODEL GRID

Figure 13.--Example of a complex particle track for Test Case 1.

and does not converge, even when exact observations are used. The parameter estimation converges normally if this observation is omitted.

Resolution: If intermediate or additional advective-transport data are available, use these in the parameter estimation as well. Otherwise, omit the advective-transport observation. It may be possible to include the observation later in the calibration when the model more accurately represents the actual system.

4. Problem: Unexpected parameter values are estimated when advective-transport observations are included in the parameter estimation.

Discussion: Often, in finding the best fit to the data, the nonlinear regression will estimate parameter values that can still be considered physically reasonable but are outside the range of what was expected. This situation causes the modeler to reexamine the range of reasonable values and determine whether the unexpected values are unreasonable.

Resolution: If the parameter values are truly unreasonable, see Problem 5.

5. Problem: Unreasonable parameter values are estimated when advective-transport observations are included in the parameter estimation. This problem is also discussed by Hill (1992, p. 226), but is included here because of its prevalence and importance.

Discussion: As demonstrated by Poeter and Hill (1996), the estimation of unreasonable parameter values by regression provides information about likely model accuracy and data accuracy and sufficiency. When advective-transport observations are included in the regression, they may provide information that is different than other types of data and sometimes conflicts with that data, as illustrated in Test Case 2. One reason for this is that heads and flows are measured at discrete points in time and reflect aquifer conditions at those points in time. Advective-transport observations reflect time-averaged aquifer conditions over the time of contaminant transport. So, by definition, they provide information about the system at different times, and when used separately may result in very different estimated parameter values.

Resolution: Parameter estimation merely provides the best fit to the available data with a given model setup. Scrutinize the sources of available data, including information such as in what season the data were observed, to determine whether the data are correctly interpreted and that the statistic used to calculate the weight correctly represents likely

41

data error. If unreasonable parameter values still cannot be explained then the conceptual model may be flawed. Reevaluate the conceptual model and revise the model accordingly.

REFERENCES CITED

Ahmed, S., de Marsily, G., and Talbot, A., 1988, Combined use of hydraulic and electrical properties of an aquifer in a geostatistical estimation of transmissivity: Ground Water, v. 26(1), p. 78-86.

Anderman, E.R., Hill, M.C., and Poeter, E.P., 1996, Two-dimensional advective transport in ground-water flow parameter estimation: Ground Water, v. 34(6), p. 1001-1009.

Carrera, J. and Neuman, S.P., 1986a, Estimation of aquifer parameters under transient and steady state conditions: 1. Maximum likelihood method incorporating prior information: Water Resources Research, v. 22(2), p. 199-210.

Carrera, J. and Neuman, S.P., 1986b, Estimation of aquifer parameters under transient and steady state conditions: 2. Uniqueness, stability, and solution algorithms: Water Resources Research, v. 22(2), p. 211-227.

Carrera, J. and Neuman, S.P., 1986c, Estimation of aquifer parameters under transient and steady state conditions: 3. Application to synthetic and field data: Water Resources Research, v. 22(2), p. 228-242.

Cheng, J-M. and Yeh, W.W-G., 1992, A proposed quasi-newton method for parameter identification in a flow and transport system: Advances in Water Resources, v. 15, p. 239-249.

Christiansen, H., Hill, M.C., Rosbjerg, D., and Jensen, K.H., 1995, Three-dimensional inverse modeling using heads and concentrations at a Danish landfill: in Proceedings of IAHS-IUGG XXI General Assembly, July, 1995, Boulder, Colorado, Wagner, B. and Illangesekare, T., eds., IAHS Pub No. 27, p. 167-175.

Cooley, R.L. and Naff, R.L., 1990, Regression modeling of ground-water flow: U.S. Geological Survey Techniques in Water Resources Investigations Chapter B4 Book 3, 232 p.

Domenico, P.A. and Schwartz, F.W., 1990, Physical and chemical hydrogeology: John Wiley & Sons, New York, 824 p.

Doussan, C., Toma, A., Paris, B., Poitevin, G., Ledoux, E., and Detay, M., 1994, Coupled use of thermal and hydraulic head data to characterize river-groundwater exchanges: Journal of Hydrology, v. 153, p. 215-229.

Draper, N.R. and Smith, H., 1981, Applied Regression Analysis: John Wiley & Sons, New York, 709 p.

Graybill, F.A., 1976, Theory and Application of The Linear Model: Wadsworth & Brooks, Pacific Grove, CA, 704 p.

Harvey, C.F. and Gorelick, S.M., 1995, Mapping hydraulic conductivity: Sequential conditioning with measurements of solute arrival time, hydraulic head, and local conductivity: Water Resources Research, v. 31(7), p. 1615-1626.

Hess, K.M., Wolf, S.H., and Celia, M.A., 1992, Large-scale natural gradient tracer test in sand and gravel, Cape Cod, Massachusetts 3. Hydraulic conductivity variability and calculated macrodispersivities: Water Resources Research, v. 28(8), p. 2011-2027.

Hill, M.C., 1992, A computer program (MODFLOWP) for estimating parameters of a transient, three-dimensional, ground-water flow model using nonlinear regression: U.S. Geological Survey Open-File Report 91-484, 358 p.

Hill, M.C., 1994, Five computer programs for testing weighted residuals and calculating linear confidence and prediction intervals on results from the ground-water parameter-estimation computer program MODFLOWP: U.S. Geological Survey Open-File Report 93-481, 81 p.

Hyndman, D.W. and Gorelick, S.M., 1996, Estimating lithologic and transport properties in three dimensions using seismic and tracer data: The Kesterson aquifer: Water Resources Research, v. 32(9), p. 2659-2670.

Keidser, A. and Rosbjerg, D., 1991, A comparison of four inverse approaches to ground-water flow and transport parameter identification: Water Resources Research, v. 27(9), p. 2219-2232.

LaVenue, M., Andrews, R.W., and Ramarao, B.S., 1989, Groundwater travel time uncertainty analysis using sensitivity derivatives: Water Resources Research, v. 25(7), p. 1551-1566.

LeBlanc, D.R., 1984a, Digital model of solute transport in a plume of sewage contaminated ground water: in LeBlanc, D.R., ed., 1984, Movement and Fate of Solutes in a Plume of Sewage-Contaminated Water, Cape Cod, Massachusetts, U.S. Geological Survey Toxic Waste Ground-Water Contamination Program: U.S. Geological Survey Open-File Report 84-475..

LeBlanc, D.R., 1984b, Sewage plume in a sand and gravel aquifer, Cape Cod, Massachusetts: U.S. Geological Survey Water-Supply Paper 2218, 28 p.

LeBlanc, D.R., Garabedian, S.P., Hess, K.M., Gelhar, L.W., Quadri, R.D., Stollenwerk, K.G., and Wood, W.W., 1991, Large-scale natural gradient tracer test in sand and gravel, Cape Cod, Massachusetts 1. Experimental design and observed tracer movement: Water Resources Research, v. 27(5), p. 895-910.

McDonald, M.G. and Harbaugh, A.W., 1988, A modular three-dimensional finite difference ground-water flow model: U.S. Geological Survey Techniques in Water Resources Investigations, Chapter A1, Book 6.

McDonald, M.G., Harbaugh, A.W., Orr, B.R., and Ackerman, D.J., 1992, A method of converting no-flow cell to variable-head cells in the U.S. Geological Survey modular finite-difference ground-water flow model: U.S. Geological Survey Open-File Report 91-536, 99 p.

Medina, A. and Carrera, J., 1996, Coupled estimation of flow and solute transport parameters: Water Resources Research, v. 32(10), p. 3063-3076.

Poeter, E.P. and Gaylord, D.R., 1990, Influence of aquifer heterogeneity on contaminant transport at the Hanford Site: Ground Water, v., 28(6), p. 900-909.

Poeter, E.P. and Hill, M.C., 1996, Unrealistic parameter estimates in inverse modeling: A problem or benefit for model calibration: in Calibration and Reliability in Groundwater Modeling (Proceedings of the ModelCARE 96 Conference held at Golden, Colorado, September 1996), IAHS Publ. No. 237, p. 277-285.

Pollock, D.W., 1989, Documentation of computer programs to compute and display pathlines using results from the U.S. Geological Survey modular three-dimensional finite-difference ground-water flow model: U.S. Geological Survey Open-File Report 89-381, 188 p.

Strecker, E.W. and Chu, W., 1986, Parameter identification of a ground-water contaminant transport model: Ground Water, v. 24(1), p. 56-72.

Sun, N-Z., 1994, Inverse problems in groundwater modeling: Klewer, Boston, 337 p.

Sun, N-Z. and Yeh, W.W-G., 1990a, Coupled inverse problems in groundwater modeling, 1. Sensitivity analysis and parameter identification: Water Resources Research, v., Vol. 26, No. 10, pp. P. 2507-2525.

Sun, N-Z. and Yeh, W.W-G., 1990b, Coupled inverse problems in groundwater modeling, 2. Identifiability and experimental design: Water Resources Research, v. 26(10), p. 2527-2540.

Sykes, J.F. and Thomson, N.R., 1988, Parameter identification and uncertainty analysis for variably saturated flow: Advances in Water Resources, v. 11, p. 185-191.

Wagner, B.J. and Gorelick, S.M., 1987, Optimal groundwater quality management under parameter uncertainty: Water Resources Research, v. 23(7), p. 1162-1174.

Weiss, R. and Smith, L., 1993, Parameter estimation using hydraulic head and environmental tracer data: in Poeter, E.P., Ashlock, S., and Proud, J., ed., 1993, IGWMC Ground Water Modeling Conference, Golden, Co., 1993, Colorado School of Mines.

Wexler, E.J., 1992, Analytical solutions for one-, two-, and three-dimensional solute transport in ground-water systems with uniform flow: U.S. Geological Survey Techniques in Water Resources Investigations, Chapter B7, Book 3, 190 p.

Woodbury, A.D. and Smith, L., 1988, Simultaneous inversion of hydrogeologic and thermal data 2. Incorporation of thermal Data: Water Resources Research, v. 24(3), p. 356-372.

Xiang, Y., Sykes, J.F., and Thomson, N.R., 1993, A composite L1 parameter estimator for model fitting in ground-water flow and solute transport simulation: Water Resources Research, v. 29(6), p. 1661-1673.

Yeh, W.W-G., 1986, Review of parameter identification procedures in groundwater hydrology: The inverse problem: Water Resources Research, v. 22(2), p. 95-108.

Zheng, C., 1994, Analysis of particle tracking errors associated with spatial discretization: Ground Water, v. 32(5), p. 821-828.

APPENDIX A: ADV INPUT AND OUTPUT

The Advective-Transport Observation Package allows users of MODFLOWP to include advective-transport measurements as observations in nonlinear regression.   Advective-transport observations as used here are characterized by specified source locations and subsequent advective-transport locations measured at known times, or specified final locations and previous locations measured at known times. In the first option, advective transport is simulated forward in time; in the second, it is simulated backward in time.   The observed locations can be estimated directly from concentration data from either continuous or slug sources.   Use of advective-transport observations provides important constraints when calibrating a ground-water flow model and, if applicable, the resulting parameter values can be used as improved estimates in the construction of a contaminant transport model.

The Advective-Transport Observation Package includes new subroutines ADV1RP, ADV1P, SADV1L, SADV1S, SADV1WR, and ADV1O, and is invoked by specifying the unit number of the ADV input file as IOUADV, which is read in I5 format from columns 61-65 on line 7 of the MODFLOWP input file described by Hill (1992, p. 132 and RELEASE NOTES for revisions 2.13 and later). The first line of the ADV input file contains information about the number of advective-transport observations and a flag controlling the particle tracking that is necessary to dimension the appropriate arrays.

The Advective-Transport Observation Package allows the user to specify any number of intermediate observation points along each advective-transport path, thus allowing information about the path of travel to be included in the regression. The number of points and the initial location of the particle track are specified in DATA SET 5. The location of each of the observed advective-front observations, statistics used to calculate the weights of the observations, and the time of the observation are entered in repetitions of DATA SET 5A. DATA SETS 5 and 5A are repeated as a group for each of the NPTH advective-transport path observations. DATA SET 6 contains data for the full weight matrix, should the user wish to use it; ensure that IOUWTQ is set to the appropriate value to use this option. The format for these data sets is shown below.

ADV Input File

LINE	COLUMN	FORMAT	VARIABLE	DEFINITION

Line 1 specifies values needed to dimension arrays.

LINE	COLUMN	FORMAT	VARIABLE	DEFINITION
1	1-5	I5	NPTH	The number of advective-transport paths that will be used (i.e. the total number of DATA SETS 5).
	6-10	I5	NTT2	The total number of advective-transport observation locations that will be used (i.e. the total number of DATA SETS 5A).
	11-15	I5	IOUTT2	Output unit number for particle-tracking positions.
	16-20	I5	KTFLG	A flag indicating how the particle-tracking time step is calculated; if equal to 1, particles are displaced from one cell face to the next; if equal to 2, particles are displaced using time steps specified by ADVSTP on this line; if equal to 3, both of the above are included.
	20-25	I5	KTREV	A flag indicating the direction of particle displacement; if equal to 1, particles are displaced in a forward direction; if equal to -1, particles are displaced in a backward direction.
	26-30	I5	NCLAY	The number of confining layers that have been represented in VCONT arrays.
	31-35	F10.0	ADVSTP	The time-step length to be used in particle-tracking options 2 and 3.

DATA SET	NUMBER OF LINES	FORMAT	VARIABLE	DEFINITION

DATA SET 1 identifies where confining units occur. Omit DATA SET 1 if NCLAY=0 on LINE 1 of this INPUT FILE.

1	1 or more	16I5	LAYC(K),K= 1,NCLAY	Layer numbers below which the confining layers apply. The order of the confining layers corresponds to the order of the thickness arrays in DATA SET 3.

DATA SET 2 contains an array of the elevation of the top of the top layer and must be included in the ADV INPUT FILE if there is more than one layer in the model.

2		1 NROWxNCOL array. Read by using module U2DREL of McDonald and Harbaugh (1988, p. 14-26 to 14-29; E-1).

DATA SET 3 contains arrays of the thicknesses of confining layers. Omit if NCLAY=0 on LINE 1.

3		NCLAY (LINE 1) NROWxNCOL arrays. Read by using module U2DREL of McDonald and Harbaugh (1988, p. 14-26 to 14-29; E-1).

DATA SET 4 contains arrays of the porosity of each of the model layers, including possible confining layers, and must be included in the ADV INPUT FILE.

4		NLAY+NCLAY NROWxNCOL arrays. Read by using module U2DREL of McDonald and Harbaugh (1988, p. 14-26 to 14-29; E-1).

DATA SET	NUMBER OF LINES	FORMAT	VARIABLE	DEFINITION

DATA SETS 5 and 5A are repeated as a group for each of the NPTH advective-transport observation paths. These DATA SETS must be included in the ADV INPUT FILE.

DATA SET	NUMBER OF LINES	FORMAT	VARIABLE	DEFINITION
5	1	4I5,	NPNT, SLAY, SROW, SCOL	Number of points along this path (i.e. the number of repetitions of DATA SET 5A that follow); layer, row, and column of initial particle position;
		3F5.0,	LOFF, ROFF, COFF	Layer, row, and column offsets used to locate the initial position within the cell (must range between -0.5 and 0.5; see fig. 6 of Hill (1992, p. 22));
5A	NPNT	A4, 1X, 3I5	DID, LAY, ROW, COL	Data identifier; layer, row, and column of advective-transport observation;
		3F5.0	LOFF, ROFF, COFF	Layer, row, and column offsets used to locate the advective-transport observation within the cell (must range between -0.5 and 0.5; see fig. 6 of Hill (1992, p. 22));
		3(F5.0,I3)	XSTAT, IXSTAT, YSTAT, IYSTAT, ZSTAT, IZSTAT	Each pair of numbers represents the value from which the weight of the observed location is calculated, and a flag to indicate whether the value is a variance (0), a standard deviation (1), or a coefficient of variation (2) (see Hill (1992) p. 143);
		F10.0	TT2	The time of this advective-front observation, relative to the beginning of the simulation, in consistent units.

DATA SETS 6 and 6A contain information to be used in the full weight matrix. These DATA SETS must be included in the ADV INPUT FILE if IOUWTQ on line 7 of the MODFLOWP INPUT FILE is greater than 0.

DATA SET	NUMBER OF LINES	FORMAT	VARIABLE	DEFINITION
6	1	A20, I5	FMTIN, IPRN	The format in which the array values are read and a flag indicating whether the array should be printed;
6A	I=1,NTT2	FMTIN	WTQ(I,J), J=1,NTT2	The error variance-covariance matrix. Along the diagonals (i=j) the variances are specified; off diagonals (i≠j) are the covariances between advective-transport observations i and j.

The following ADV input file is an example of the file used for Test Case 1.

```
    2    2   00    1    1    0      0.0                              LINE 1
       42        1.0 (12f8.2)                      2                 DATA SET 2
    0.00  466.66  970.89  979.17  979.48  980.07 1025.00 1123.69 1184.28 1185.76 1186.51 9999.00
 9999.00 9999.00 9999.00 9999.00 9999.00 9999.00
    0.00  460.53  968.83  979.02  979.21  979.77 1015.11 1103.04 1170.61 1186.49 1187.26 1188.65
 9999.00 9999.00 9999.00 9999.00 9999.00 9999.00
    0.00  432.95  961.24  973.60  978.55  957.74  987.47 1088.84 1179.69 1186.78 1187.39 1190.05
 1191.79 9999.00 9999.00 9999.00 9999.00 9999.00
    0.00  291.69  752.49  967.22  971.47  964.35  990.43 1082.56 1176.54 1177.24 1159.66 1192.36
 1193.54 1194.92 9999.00 9999.00 9999.00 9999.00
    0.00  220.86  552.04  799.15  897.53  929.42  956.07  983.73 1077.55 1147.71 1154.33 1194.15
 1195.09 1196.29 1197.29 9999.00 9999.00 9999.00
    0.00  188.80  463.00  692.59  852.09  892.57  932.76  906.94 1007.63 1147.73 1201.15 1195.77
 1196.37 1197.88 1198.28 1198.34 9999.00 9999.00
   27.65  189.71  420.51  653.17  857.06  922.11 1014.73  951.16 1023.76 1183.96 1259.68 1242.39
 1215.40 1200.60 1200.03 1198.83 1197.33 9999.00
   50.33  209.99  431.34  642.47  850.77  944.38 1014.46  953.31 1036.80 1233.05 1337.05 1346.38
 1256.78 1205.05 1203.72 1200.92 1197.30 1100.00
   67.18  233.93  444.97  634.74  835.28  925.80  971.05  931.50 1049.61 1275.58 1407.16 1449.87
 1356.59 1209.95 1209.11 1204.70 1176.94 1100.00
   77.44  262.59  462.38  635.42  812.44  951.31  990.28  999.73 1107.81 1286.30 1395.35 1453.25
 1424.78 1276.80 1214.27 1202.18 1159.09 1100.00
  207.65  336.39  484.48  640.95  809.63  926.59  996.19 1045.80 1129.56 1312.27 1441.08 1456.96
 1447.99 1315.52 1217.30 1204.81 1157.15 1100.00
 9999.00 9999.00 9999.00 9999.00  871.62  949.88 1018.16 1062.88 1036.73 1312.10 1459.70 1459.79
 1479.20 1375.99 1284.80 1218.50 1164.71 1100.00
 9999.00 9999.00 9999.00 9999.00 9999.00 1000.38 1063.05 1123.83 1184.97 1336.58 1482.97 1513.53
 1515.39 1419.18 1314.91 1228.81 1181.96 1153.66
 9999.00 9999.00 9999.00 9999.00 9999.00 9999.00 1117.51 1183.17 1225.02 1283.48 1375.39 1404.99
 1388.08 1333.35 1276.05 1215.86 1193.01 1177.67
 9999.00 9999.00 9999.00 9999.00 9999.00 9999.00 9999.00 1239.21 1241.07 1242.52 1282.86 1303.60
 1286.91 1219.00 1240.73 1206.68 1193.28 1188.76
 9999.00 9999.00 9999.00 9999.00 9999.00 9999.00 9999.00 9999.00 1241.55 1242.06 1255.55 1262.52
 1249.10 1206.20 1216.15 1197.47 1193.35 1192.28
 9999.00 9999.00 9999.00 9999.00 9999.00 9999.00 9999.00 9999.00 9999.00 1242.22 1246.68 1247.25
 1238.52 1221.48 1209.43 1195.85 1194.18 1193.66
 9999.00 9999.00 9999.00 9999.00 9999.00 9999.00 9999.00 9999.00 9999.00 9999.00 1244.51 1242.16
 1234.80 1222.75 1208.12 1195.45 1194.60 1194.10
         0        0.3                                              DATA SET 4
         0        0.3                                              DATA SET 4
         0        0.3                                              DATA SET 4
     1    1   14   11  0.5  0.0  0.0                               DATA SET 5
 L_1     1   12    5  0.5-0.09-0.131500.  11500.  1 750.  1   5.59e+8  DATA SET 5A
     1    1   13   12  0.5  0.0  0.0                               DATA SET 5
 C_1     1   10   11 0.48-0.37-0.351500.  11500.  1 750.  1   2.28e+6  DATA SET 5A
```

Output from ADV

Because the Advective-Transport Observation Package fits into the general framework of MODFLOWP, output is interspersed in the appropriate places throughout the MODFLOWP output. The places where this occurs are:

- The initial position and time and location of the observed position are printed after the flow observation information.

- At the first parameter-estimation iteration, the simulated row, column, x-, y-, and z-positions, average velocity in that particle step, and x-, y-, and z-sensitivities to the parameters at each particle step are printed for each of the parameters.

- The advective-transport observation residuals, contribution to the sum of the squared weighted residuals, and scaled sensitivities are printed for the first and final parameter-estimation iterations in the appropriate locations with the other observations.

- The advective-transport residuals are included in the list of ordered residuals and normality calculation at the end of the printout.

An example of the excerpted output file for Test Case 1 is included below. The ADV package output appears in bold type and three dots (...) indicates omitted output.

```
UNIT 7 IS USED FOR A FILE NAMED FILES

 FILENAME=d:\Evan\Yucca\Ymp\adv.2          UNIT=   2  BIN=
 FILENAME=d:\Evan\Yucca\Ymp\basp           UNIT=   1  BIN=
 FILENAME=d:\Evan\Yucca\Ymp\welp           UNIT=  12  BIN=
 FILENAME=d:\Evan\Yucca\Ymp\shd            UNIT=  -4  BIN=
 FILENAME=d:\Evan\Yucca\Ymp\bcfp           UNIT=  11  BIN=
 FILENAME=d:\Evan\Yucca\Ymp\evt            UNIT=  15  BIN=
 FILENAME=d:\Evan\Yucca\Ymp\ghb            UNIT=  17  BIN=
 FILENAME=d:\Evan\Yucca\Ymp\drn            UNIT=  13  BIN=
 FILENAME=d:\Evan\Yucca\Ymp\rch            UNIT=  18  BIN=
 FILENAME=d:\Evan\Yucca\Ymp\pcg2p          UNIT=  23  BIN=
 FILENAME=d:\Evan\Yucca\Ymp\out            UNIT=  22  BIN=
 FILENAME=d:\Evan\Yucca\Ymp\par.tru        UNIT=  25  BIN=
 FILENAME=d:\Evan\Yucca\Ymp\hobsc.out      UNIT=  40  BIN=
 FILENAME=d:\Evan\Yucca\Ymp\qobsc.out      UNIT=  41  BIN=
 FILENAME=d:\Evan\Yucca\Ymp\adv.out        UNIT=  42  BIN=
 FILENAME=d:\Evan\Yucca\Ymp\t.2            UNIT=  38  BIN=
 FILENAME=d:\Evan\Yucca\Ymp\zones          UNIT=  39  BIN=
 FILENAME=d:\Evan\Yucca\Ymp\b              UNIT= -33  BIN=
 FILENAME=d:\Evan\Yucca\Ymp\bin            UNIT= -49  BIN=bin

SUCCESSFULLY OPENED   17 FILES


               MODFLOWP VERSION 2.12  07JUNE1996

1           U.S. GEOLOGICAL SURVEY MODULAR FINITE-DIFFERENCE GROUND-WATER MODEL  - MODFLOWP VERSION
0MODFLOWP SIMULATION OF MODFLOWP TEST CASE 1
    3 LAYERS      18 ROWS      18 COLUMNS
    1 STRESS PERIOD(S) IN SIMULATION
 MODEL TIME UNIT IS SECONDS
0I/O UNITS:
 ELEMENT OF IUNIT:   1  2  3  4  5  6  7  8  9 10 11 12 13 14 15 16 17 18 19 20 21 22 23 24
        I/O UNIT:  11 12 13  0 15  0 17 18  0  0 22 23  0 25  0  0  0  0  0  0  0  0  0  0
0BAS1 -- BASIC MODEL PACKAGE, VERSION 1, 9/1/87 INPUT READ FROM UNIT  1
 ARRAYS RHS AND BUFF WILL SHARE MEMORY.
 START HEAD WILL BE SAVED
     9444 ELEMENTS IN X ARRAY ARE USED BY BAS
     9444 ELEMENTS OF X ARRAY USED OUT OF 1000000
0BCF2 -- BLOCK-CENTERED FLOW PACKAGE, VERSION 2, 7/1/91 INPUT READ FROM UNIT 11
 STEADY-STATE SIMULATION
 HEAD AT CELLS THAT CONVERT TO DRY=       .00000
 WETTING CAPABILITY IS NOT ACTIVE
     LAYER AQUIFER TYPE
     ------------------
       1       0
       2       0
       3       0
     3 ELEMENTS IN X ARRAY ARE USED BY BCF
 ...

 NUMBER OF PIDS DISTRIBUTED AS LOG-TRANSFORM VALUES.:         0

 ADVECTIVE-TRANSPORT OBSERVATION FILE UNIT NO ........     42
 NUMBER OF PARTICLES ................................      2
 TOTAL NUMBER OF ADVECTIVE-TRANSPORT OBSERVATIONS ...      2
 OUTPUT UNIT NUMBER FOR ADVECTIVE-TRANSPORT INFO ....      0

 TWO- OR THREE-DIMENSIONAL TRACKING (KTDIM)..........      3
 PARTICLE-TRACKING TIME-STEP FLAG (KTTFLG)...........      1
 TIME STEP (IF KTTFLG>1).............................  .00000000
 FORWARD OR BACKWARD PARTICLE TRACKING (KTREV).......      1
 NUMBER OF CONFINING LAYERS .........................      0

  11489 ELEMENTS IN X ARRAY ARE USED FOR SENSITIVITIES
  29796 ELEMENTS OF X ARRAY USED OUT OF1000000
0PARI -- PARAMETER ESTIMATION PACKAGE, VERSION 1, 12/01/91
 ...

 GROUP# 10, BOUNDARY TYPE  4, # OF FLOWS    1, # OF CELLS IN GROUP    -1
                                                   STREAMFLOW
 OBS#  ID    TIME  STEP AND OFFSET    OBSERVED      GAIN(-) OR   STATISTIC
                                                   LOSS(+)
  52  DRN1    0        .00            -6.20         .300
```

52

```
LAYER  ROW  COLUMN   FACTOR
  1.   16.    14.      1.00
```

ADVECTIVE-TRANSPORT OBSERVATION DATA

0

ELEVATION OF TOP LAYER FOR LAYER 1 WILL BE READ ON UNIT 42 USING FORMAT: (12f8.2)

```
        1        2        3        4        5        6        7        8        9
       10       11       12       13       14       15       16       17       18
...............................................................................................
0  1  .000000  466.660  970.890  979.170  979.480  980.070  1025.00  1123.69  1184.28
0  2  1185.76  1186.51  9999.00  9999.00  9999.00  9999.00  9999.00  9999.00  9999.00
0  3  .000000  460.530  968.830  979.020  979.210  979.770  1015.11  1103.04  1170.61
0  4  1186.49  1187.26  1188.65  9999.00  9999.00  9999.00  9999.00  9999.00  9999.00
0  5  .000000  432.950  961.240  973.600  978.550  957.740  987.470  1088.84  1179.69
0  6  1186.78  1187.39  1190.05  1191.79  9999.00  9999.00  9999.00  9999.00  9999.00
0  7  .000000  291.690  752.490  967.220  971.470  964.350  990.430  1082.56  1176.54
0  8  1177.24  1192.36  1194.92  1193.54  9999.00  9999.00  9999.00  9999.00  9999.00
0  9  .000000  220.860  552.040  799.150  897.530  929.420  956.070  983.730  1077.55
0 10  1147.71  1154.33  1194.15  1195.09  1196.29  1197.29  9999.00  9999.00  9999.00
0 11  .000000  188.800  463.000  692.590  852.090  892.570  932.760  906.940  1007.63
0 12  1147.73  1201.15  1195.77  1196.37  1197.88  1198.28  1198.34  9999.00  9999.00
0 13  27.6500  189.710  420.510  653.170  857.060  922.110  1014.73  951.160  1023.76
0 14  1183.96  1259.68  1242.39  1215.40  1200.60  1200.03  1198.83  1197.33  9999.00
0 15  50.3300  209.990  431.340  642.470  850.770  944.380  1014.46  953.310  1036.80
0 16  1233.05  1337.05  1346.38  1256.78  1205.05  1203.72  1200.92  1197.30  1100.00
0 17  67.1800  233.930  444.970  634.740  835.280  925.800  971.050  931.500  1049.61
0 18  1275.58  1407.16  1449.87  1356.59  1209.95  1209.11  1204.70  1176.94  1100.00

      77.4400  262.590  462.380  635.420  812.440  951.310  990.280  999.730  1107.81
      1286.30  1395.25  1453.25  1424.78  1276.80  1214.27  1202.18  1159.09  1100.00
      207.650  336.390  484.480  640.950  809.630  926.590  996.190  1045.80  1129.56
      1312.27  1441.08  1456.96  1447.99  1315.52  1217.30  1204.81  1157.15  1100.00
      9999.00  9999.00  9999.00  9999.00  871.620  949.880  1018.16  1062.88  1036.73
      1312.10  1459.79  1459.70  1479.20  1375.99  1284.80  1218.50  1164.71  1100.00
      9999.00  9999.00  9999.00  9999.00  9999.00  1000.38  1063.05  1123.83  1184.97
      1336.58  1482.97  1513.53  1515.39  1515.99  1419.18  1314.91  1228.81  1181.96  1153.66
      9999.00  9999.00  9999.00  1388.08  1333.35  1276.05  1215.86  1193.01  1177.67
      1375.39  1404.99  9999.00  9999.00  9999.00  9999.00  9999.00  1239.21  1241.07
      1283.48  1404.99  1388.08  1286.91  1219.00  1240.73  1206.68  1193.28  1188.76
      1242.52  1282.86  1303.60  9999.00  9999.00  9999.00  9999.00  9999.00  1241.55
      1242.06  1242.52  1249.10  1206.20  1216.15  1197.47  1193.35  1192.28
      1255.55  1262.52  9999.00  9999.00  9999.00  9999.00  9999.00  9999.00
      1246.68  1247.25  1238.52  1221.48  1209.43  1195.85  1194.18  1193.66
      9999.00  9999.00  9999.00  9999.00  1222.75  1208.12  1195.45  1194.60
      1244.51  1242.16  1234.80
```

```
0           POROSITY OF LAYER =  .3000000    FOR LAYER   1
0           POROSITY OF LAYER =  .3000000    FOR LAYER   2
0           POROSITY OF LAYER =  .3000000    FOR LAYER   3
```

3D PARTICLE TRACKING USED IN ALL LAYERS

```
   PATH # 1 INITIAL LOCATION
 LAYER  ROW  COL   LOFF    ROFF    COFF
 -----  ---  ---   ----    ----    ----
   1    14   11    .50     .00     .00
```

OBSERVED INTERMEDIATE PATH LOCATION(S)
```
 OBS # ID    TIME    LAY RW COL LOFF ROFF COFF | X     WEIGHT   TYPE| Y       WEIGHT   TYPE| Z     WEIGHT   TYPE
 -----------------------------------------------------------------------------------------------------------------
53- 55 L_1  .5590E+09  1 12  5  .50 -.09 -.13  6555.00 .2250E+07  1 17115.00 .2250E+07  1  871.62 .5625E+06  1
```

```
   PATH # 2 INITIAL LOCATION
 LAYER  ROW  COL   LOFF    ROFF    COFF
 -----  ---  ---   ----    ----    ----
   1    13   12    .50     .00     .00
```

OBSERVED INTERMEDIATE PATH LOCATION(S)
```
 OBS # ID    TIME    LAY RW COL LOFF ROFF COFF | X     WEIGHT   TYPE| Y       WEIGHT   TYPE| Z     WEIGHT   TYPE
 -----------------------------------------------------------------------------------------------------------------
```

56- 58 C_1 .2280E+07 1 10 11 .48 -.37 -.35 15225.00 .2250E+07 1 13695.00 .2250E+07 1 1385.35 .5625E+06 1

REGRESSION DATA (DATA SETS 13 A, B, C, AND D):

...

```
          ENTERING PARTICLE TRACKING ROUTINE (ADV1P)
-------------------------------------------------------------
SUBROUTINE (ADV1P) IS HARDWIRED WITH THE FOLLOWING OPTIONS:
LINEAR VELOCITY INTERPOLATION (SADV1LL)
SEMI-ANALYTICAL PARTICLE TRACKING (SADV1S)
PARTICLE NO.    1 ABOVE WATER TABLE - MOVED TO WATER TABLE (ADV1P)
```

ADVECTIVE-TRANSPORT OBSERVATION NUMBER   1
PARTICLE TRACKING LOCATIONS AND TIMES:

OBS #	ID	LAYER	ROW	COL	X-POSITION	Y-POSITION	Z-POSITION	X-VELOCITY	Y-VELOCITY	Z-VELOCITY	VELOCITY	TIME
		1	14	11	.1575000E+05	.2025000E+05	.1371223E+04	.0000000E+00	.0000000E+00	.0000000E+00	.0000000E+00	.0000000E+00
		1	15	11	.1530753E+05	.2100000E+05	.1282849E+04	-.1208702E+04	.3056035E-04	-.7905995E-10	.2727142E-04	.3209459E+08
		1	15	10	.1500000E+05	.2134469E+05	.1242509E+04	-.1311329E-04	-.1740444E-04	-.8959638E-11	.2144943E-04	.5371277E+08
		1	15	9	.1350000E+05	.2212159E+05	.1241061E+04	-.1539909E-04	-.1246126E-04	-.3420940E-10	.2308509E-04	.1268879E+09
		1	15	8	.1200000E+05	.2146797E+05	.1239199E+04	-.2661645E-04	-.1573919E-04	-.2770701E-10	.3270966E-04	.1769105E+09
		1	14	8	.1132171E+05	.2100000E+05	.1183157E+04	-.3362949E-04	-.1437606E-04	-.9099319E-10	.3076885E-04	.2037548E+09
		1	14	7	.1050000E+05	.1970347E+05	.1117493E+04	-.9403000E-05	-.2089481E-04	-.4105425E-10	.1977702E-04	.2814404E+09
		1	13	7	.1027046E+05	.1950000E+05	.1063033E+04	-.1184557E-04	-.8986837E-05	-.1647223E-10	.1481311E-04	.3024715E+09
		1	13	6	.9000000E+04	.1828759E+05	.1000362E+04	-.1043145E-04	-.1039721E-04	-.4461937E-11	.1463372E-04	.4225538E+09
		1	12	6	.8696320E+04	.1800000E+05	.9498618E+03	-.1072981E-04	-.8160540E-05	-.7581942E-11	.1332162E-04	.4541780E+09
		1	12	5	.7500000E+04	.1714620E+05	.8716011E+03	-.1171504E-04	-.1009630E-04	-.7763043E-11	.1570629E-04	.5478786E+09
53- 55	L_1	1	12	5	.7353439E+04	.1705882E+05	.8716010E+03	-.1387855E-04	-.7486235E-05	-.9155754E-11	.1535499E-04	.5590000E+09

AVERAGE PARTICLE VELOCITY ALONG PATH: .19963020E-04

ADVECTIVE-TRANSPORT OBSERVATION NUMBER   2
PARTICLE TRACKING LOCATIONS AND TIMES:

OBS #	ID	LAYER	ROW	COL	X-POSITION	Y-POSITION	Z-POSITION	X-VELOCITY	Y-VELOCITY	Z-VELOCITY	VELOCITY	TIME
		1	13	12	.1725000E+05	.1875000E+05	.1513530E+04	.0000000E+00	.0000000E+00	.0000000E+00	.0000000E+00	.0000000E+00
		1	12	12	.1705103E+05	.1800000E+05	.1154973E+04	-.3021150E-03	-.8552607E-03	-.7733334E-03	.1426685E-02	.5991388E+06
		1	11	12	.1692045E+05	.1650000E+05	.1043615E+04	-.2889241E-03	-.1755260E-02	-.3090333E-03	.3003962E-02	.1101737E+07
		1	11	12	.1681934E+05	.1500000E+05	.1006773E+04	-.3333564E-03	-.4685779E-02	-.1454238E-03	.5377766E-02	.1381380E+07
		1	10	11	.1650000E+05	.1387795E+05	.9327993E+03	-.1388785E-02	-.6104663E-02	-.9703868E-04	.6129397E-02	.1572093E+07
56- 58	C_1	1	10	11	.1557580E+05	.1385079E+05	.1028538E+04	-.1996869E-02	-.4815448E-04	-.6222471E-04	.1313089E-02	.2280000E+07

AVERAGE PARTICLE VELOCITY ALONG PATH: .26170710E-02

ALL PARTICLES MOVED EXITING (ADV1P)

...

ADVECTIVE-TRANSPORT OBSERVATIONS

OBS#	ID		OBSERVED LOCATION	CALCULATED LOCATION	RESIDUAL	WEIGHT **0.5	WEIGHTED RESIDUAL
53	L_1	X =	6555.00	7353.44	-798.44	.00067	-.53
54	L_1	Y =	17115.00	17058.82	56.18	.00067	.04
55	L_1	Z =	871.62	871.60	.02	.00133	.00
56	C_1	X =	15225.00	15575.80	-350.80	.00067	-.23
57	C_1	Y =	13695.00	13850.79	-155.79	.00067	-.10
58	C_1	Z =	1385.35	1028.54	356.81	.00133	.48

```
STATISTICS FOR THESE RESIDUALS
MAXIMUM WEIGHTED RESIDUAL :  .476E+00 OBS#  58
MINIMUM WEIGHTED RESIDUAL : -.532E+00 OBS#  53
AVERAGE WEIGHTED RESIDUAL : -.139E+00
# RESIDUALS >= 0. :   3
# RESIDUALS < 0. :   3
NUMBER OF RUNS :   16 IN  58 OBSERVATIONS

SUM OF SQUARED WEIGHTED RESIDUALS (ALL DEP. VAR.)   396.95

SUM OF SQUARED WEIGHTED RESIDUALS (ALL DEP. VAR.)   396.95
STATISTICS FOR ALL RESIDUALS :
AVERAGE WEIGHTED RESIDUAL :  .527E+00
# RESIDUALS >= 0. :   28
# RESIDUALS < 0. :   30
NUMBER OF RUNS :  16 IN  58 OBSERVATIONS
RUNS STATISTIC (TOO FEW RUNS):  -3.57
```

54

```
(IF #NEG>10 AND #POS>10, P(STAT < -1.28) = 0.10,
                         P(STAT < -1.645) = 0.05,
                         P(STAT < -1.96) = 0.025)
RUNS STATISTIC (TOO MANY RUNS):      -3.84
(IF #NEG>10 AND #POS>10, P(STAT > 1.28) = 0.10,
                         P(STAT > 1.645) = 0.05,
                         P(STAT > 1.96) = 0.025)


        ENTERING PARTICLE TRACKING ROUTINE (ADV1P)
------------------------------------------------------------------
SUBROUTINE (ADV1P) IS HARDWIRED WITH THE FOLLOWING OPTIONS:
LINEAR VELOCITY INTERPOLATION (SADV1L)
SEMI-ANALYTICAL PARTICLE TRACKING (SADV1S)
PARTICLE NO.   1 ABOVE WATER TABLE - MOVED TO WATER TABLE (ADV1P)
```

ADVECTIVE-TRANSPORT OBSERVATION NUMBER   1   PARAMETER #:   1 TYPE: T
PARTICLE TRACKING LOCATIONS, TIMES, AND SENSITIVITIES:
(SENSITIVITIES ARE SCALED BY CURRENT PARAMETER VALUE)

OBS # ID	LAYER ROW COL	X-POSITION	Y-POSITION	Z-POSITION	VELOCITY	TIME	X-SENSITIVITY	Y-SENSITIVITY	Z-SENSITIVITY
	1 14 11	.1575000E+05	.2025000E+05	.1371223E+04	.0000000E+00	.0000000E+00	.0000000E+00	.0000000E+00	.0000000E+00
	1 15 11	.1530753E+05	.2100000E+05	.1282849E+04	.2727142E-04	.3209459E+08	.4471932E+02	-.3521278E+02	.2205088E-03
	1 15 10	.1500000E+05	.2134469E+05	.1242509E+04	.2144943E-04	.5371277E+08	.9279276E+02	-.4857818E+02	.2011215E-03
	1 15 9	.1350000E+05	.2212159E+05	.1241661E+04	.2308509E-04	.1268879E+09	.4146276E+03	-.4362426E+03	-.6417643E-04
	1 15 8	.1200000E+05	.2146797E+05	.1239193E+04	.3270966E-04	.1769105E+09	.7866572E+03	.7604900E+02	.2306808E-03
	1 14 8	.1132171E+05	.2100000E+05	.1183157E+04	.3076885E-04	.2037548E+09	.5152826E+03	.2036550E+03	.8329591E-03
	1 14 7	.1050000E+05	.1970347E+05	.1117493E+04	.1977702E-04	.2814404E+09	.8107156E+03	.2873727E+03	.1905548E-03
	1 13 7	.1027046E+05	.1950000E+05	.1063033E+04	.1481311E-04	.3024715E+09	.7239493E+03	.3696992E+03	.2025915E-02
	1 13 6	.9000000E+04	.1800000E+05	.1000362E+04	.1463372E-04	.4225538E+09	.8190138E+03	.5689074E+03	.2411674E-02
	1 12 6	.8696320E+04	.1800000E+05	.9498618E+03	.1332162E-04	.4541780E+09	.9743524E+03	.7544360E+03	.2469823E-02
	1 12 5	.7500000E+04	.1714620E+05	.8716011E+03	.1570629E-04	.5478876E+09	.1050731E+04	.7623379E+03	.2728520E-02
53- 55 L_1	1 12 5	.7353439E+04	.1705882E+05	.8716010E+03	.1535499E-04	.5590000E+09	.9529565E+03	.8440740E+03	.2737391E-02

AVERAGE PARTICLE VELOCITY ALONG PATH: .19963020E-04

ADVECTIVE-TRANSPORT OBSERVATION NUMBER   2   PARAMETER #:   1 TYPE: T
PARTICLE TRACKING LOCATIONS, TIMES, AND SENSITIVITIES:
(SENSITIVITIES ARE SCALED BY CURRENT PARAMETER VALUE)

OBS # ID	LAYER ROW COL	X-POSITION	Y-POSITION	Z-POSITION	VELOCITY	TIME	X-SENSITIVITY	Y-SENSITIVITY	Z-SENSITIVITY
	1 13 12	.1725000E+05	.1875000E+05	.1513530E+04	.0000000E+00	.0000000E+00	.0000000E+00	.0000000E+00	.0000000E+00
	1 12 12	.1705103E+05	.1800000E+05	.1154973E+04	.1426685E-02	.5991388E+06	.3512510E+01	-.1939140E+02	.1256605E+00
	1 11 12	.1692045E+05	.1650000E+05	.1043615E+04	.3003962E-02	.1101737E+07	.1465145E+02	-.1040549E+03	.3014622E+00
	1 10 12	.1681934E+05	.1500000E+05	.1006773E+04	.5377766E-02	.1381380E+07	.2653072E+02	-.1747260E+03	.3473698E+00
	1 10 11	.1650000E+05	.1387795E+05	.9327993E+03	.6129397E-02	.1572093E+07	.4095417E+02	-.1808666E+03	.3549421E+00
56- 58 C_1	1 10 11	.1557580E+05	.1385079E+05	.1028538E+04	.1313089E-02	.2280000E+07	.1901365E+02	-.7411413E+02	.3918198E+01

AVERAGE PARTICLE VELOCITY ALONG PATH: .26170710E-02

...

SCALED SENSITIVITIES (SCALED BY B*(WT**.5))

PARAMETER # :	1	2	3	4	5	6	7	8	9	10
PARAMETER ID :	T	T	T	T	ANIV	ANIV	RCH	ETM	GHB	KDR

OBS# & ID										
1 W2L	6.03	16.2	-14.3	-2.25	9.11	.228	24.7	-3.16	-16.9	-1.95

...

OBS# & ID	1	2	3	4	5	6	7	8	9	10
53 L_1	.635	1.99	-4.81	.306	-.566E-01	-.455E-01	-2.76	-.630	.157E-01	.235
54 L_1	.563	.873	-2.68	.749E-01	.295E-01	.126E-01	-1.09	-.611	.766E-02	.793E-01
55 L_1	.365E-05	.817E-05	-.232E-04	-.304E-05	.829E-06	-.344E-06	-.117E-04	-.308E-05	.213E-07	.911E-06
56 C_1	.127E-01	.184	-.537E-01	-.622E-02	-.429E-01	.419E-03	.376	-.437E-02	.191E-02	-.434
57 C_1	-.494E-01	-.217	.205	.315E-02	-.647E-01	-.180E-02	-3.47	-.182E-01	-.121E-01	-.636E-01
58 C_1	-.522E-02	-.334E-01	-.488E-01	-.107E-01	.258E-01	.258E-02	-.502	-.847E-02	-.103E-02	.244

((SUM OF THE SQUARED VALUES)/ND)**.5
| 5.72 | 21.9 | 3.75 | 1.37 | 6.32 | .342 | 33.2 | 8.48 | 4.06 | 3.95 |

APPENDIX B: GETTING STARTED

Compiling and Loading ADV

The ADV Package can be used with MODFLOWP version 2.13 or later. MAIN of MODFLOWP (Hill, 1992) was changed substantially for the ADV Package and a description of the changes is presented in Appendix D. The following primary modules and submodules were modified for the ADV Package: SEN1AL, SEN1RP, SEN1OT, SSEN1O, and PAR1RE. There are three primary modules and three submodules included in the ADV Package and discussed in Appendix D: ADV1RP, ADV1P, ADV1O, SADV1L, SADV1S, and SADV1WR. Although in many instances the modifications are minor, problems and confusion can most easily be avoided by using the distributed version of MODFLOWP which includes all the modifications.

After substituting the new versions of MAIN, primary modules, and submodules discussed above and in Appendix C and allocating sufficient space in the X array (see next section), the model can be compiled and loaded as usual.

Portability

The ADV Package was written in standard FORTRAN 77 in a style similar to that of MODFLOW (McDonald and Harbaugh, 1988, p. A1) and MODFLOWP (Hill, 1992, p. 245). McDonald and Harbaugh (1988, appendix A) discuss portability in detail.

Space Requirements

The X-array space needed by MODFLOWP without the ADV Package is the same as that needed by MODFLOWP, as discussed by Hill (1992, Appendix B). To use the ADV Package, X-array storage needs to be increased as follows:

[See data entry instructions for LINE 1 of the ADV input file]

A. For ICLS and POFF, 3 x NPTH each.

B. For PRST, NROW x NCOL x (NLAY + NCLAY).

C. For TT2, NTT2.

D. For THCK, NROW x NCOL x (NCLAY + 1).

E. For NPNT, NPTH.

F. For LAYC, NCLAY.

G. Additionally, ND is increased by KTFLG x NTT2, which affects numerous arrays throughout MODFLOWP.

It is generally easiest to run the model and dimension the X-array larger if the program terminates prematurely due to insufficient space.

APPENDIX C: DERIVATION OF SENSITIVITY EQUATIONS

Calculation of Particle Location

The x-location of a particle at any given time equals the initial location plus the cumulative displacement up to that time. At the end of particle-tracking time step t, the x-location of the particle equals:

$$x_p^t = x_p^0 + \sum_{t=1}^{NPSTP} \Delta x_p^t \qquad (C1)$$

where

x_p^0 is the starting position of the observed path of advective transport and the particle [L],

t is the particle time-step counter

$NPSTP$ is the number of previous particle time steps, and

Δx_p^t is the particle x-displacement for time step t [L].

When the particle is in the cell at row i, column j, and layer k, particle displacement over time step Δt is calculated using the semi-analytical exponential particle-tracking method (Pollock, 1989) as:

$$\Delta x_p^t = x_p^t - x_p^{t-1} = \frac{1}{A_{x_{i,j,k}}} \left(v_{xp}^{t-1} e^{A_{x_{i,j,k}} \Delta t} - v_{x_{i,j-1/2,k}} \right) \qquad (C2)$$

$$A_{x_{i,j,k}} = \frac{v_{x_{i,j+1/2,k}} - v_{x_{i,j-1/2,k}}}{\Delta r_j} \qquad (C3)$$

where

v_{xp}^{t-1} is the linearly-interpolated x-velocity of particle p at time t-1 [L/T],

Δt is the length of time step t [T],

$v_{x_{i,j-1/2,k}}$ is the x-velocity at the left-hand face of the cell at row i, column j, and layer k [L/T],

$v_{x_{i,j+1/2,k}}$ is the x-velocity at the right-hand face of the cell at row i, column j, and layer k [L/T],

and

Δr_j is the cell width of column j [L].

To interpolate velocity linearly for any point p within cell i,j,k, it is assumed that the x-component of velocity, v_{xp}, is dependent only on its location along the x-axis relative to the location of the two cell faces perpendicular to the x-axis, and is independent of the y- or z-position within the cell. Thus, the

velocity will be continuous in the x-direction and discontinuous in the other directions. The x-component of the velocity for any point p in cell i,j,k is given as (Pollock, 1989):

$$v_{xp}^{t-1} = A_{x_{i,j,k}} \left(x_p^{t-1} - x_{i,j-1/2,k} \right) + v_{x_{i,j-1/2,k}} \qquad \text{(C4)}$$

where

v_{xp}^{t-1} is the x-component of velocity at point $x_p(t-1)$ [L/T],

x_p^{t-1} is the x-position of the particle at time step t-1, and is used to interpolate velocity to move the particle during time step t [L],

$x_{i,j-1/2,k}$ is the x-position of the left-hand cell face [L], and

$v_{x_{i,j-1/2,k}}$ is the velocity at the left-hand cell face [L/T].

The cell-face velocities are calculated as the flow rate through the cell face divided by the effective area of flow and are dependent on the change in head across the cell face and the hydraulic conductivity of the material. Derivations of the cell-face velocities and their sensitivities are given below.

Sensitivity of Particle Location

To calculate the sensitivity of particle location to a parameter, b, first note that, because x_p^0 is defined by the user, $\dfrac{\partial x_p^0}{\partial b}$ is equal to zero. Then, because differentiation and summation are linear, the sensitivity of the particle location to a parameter is calculated as the sum of the sensitivities of each of the particle displacements:

$$\frac{\partial x_p^t}{\partial b} = \sum_{t=1}^{NPSTP} \frac{\partial \Delta x_p^t}{\partial b} \qquad \text{(C5)}$$

Sensitivity of Semi-Analytical Particle Displacement

The derivative of Equation (C2) with respect to a parameter *b* is:

$$\frac{\partial \Delta x_p^t}{\partial b} = -\frac{\frac{\partial A_{x_{i,j,k}}}{\partial b}}{A_{x_{i,j,k}}^2} \left\{ v_{xp}^{t-1} e^{A_{x_{i,j,k}} \Delta t} - v_{x_{i,j-1/2,k}} \right\}$$

$$+ \frac{1}{A_{x_{i,j,k}}} \left\{ \frac{\partial v_{xp}^{t-1}}{\partial b} e^{A_{x_{i,j,k}} \Delta t} + \frac{\partial A_{x_{i,j,k}}}{\partial b} \Delta t \, v_{xp}^{t-1} e^{A_{x_{i,j,k}} \Delta t} - \frac{\partial v_{x_{i,j-1/2,k}}}{\partial b} \right\} \qquad \text{(C6)}$$

where $\dfrac{\partial \Delta t}{\partial b}$ equals zero because time is an independent variable.

<center>Sensitivity of Linear Velocity Interpolation Coefficient</center>

The derivative of $A_{x_{i,j,k}}$ in Equation (C3) with respect to any parameter b is given as:

$$\frac{\partial A_{x_{i,j,k}}}{\partial b} = \frac{1}{\Delta r_j} \left(\frac{\partial v_{x_{i,j+1/2,k}}}{\partial b} - \frac{\partial v_{x_{i,j-1/2,k}}}{\partial b} \right) \qquad \text{(C7)}$$

<center>Calculation of Linearly Interpolated Velocity and Sensitivity</center>

The sensitivity of the x-component of the interpolated velocity at any point p of Equation (C4) with respect to a parameter b is:

$$\frac{\partial v_{xp}^{t-1}}{\partial b} = \frac{\partial A_{x_{i,j,k}}}{\partial b} \left(x_p^{t-1} - x_{i,j-1/2,k} \right) + A_{x_{i,j,k}} \frac{\partial x_p^{t-1}}{\partial b} + \frac{\partial v_{x_{i,j-1/2,k}}}{\partial b} \qquad \text{(C8)}$$

<center>Calculation of Horizontal Cell-Face Velocities and Sensitivities</center>

The velocity on the left x-face of cell i,j,k is defined as the flow rate through the cell face divided by the effective area of flow:

$$v_{x_{i,j-1/2,k}} = \frac{2Q_{x_{i,j-1/2,k}}}{n_{i,j,k} \Delta c_i \left(l_{i,j-1,k} + l_{i,j,k} \right)} \qquad \text{(C9)}$$

where

<center>60</center>

$v_{x_{i,j-1/2,k}}$ is the velocity on face i,j-½,k [L/T],

$Q_{x_{i,j-1/2,k}}$ is the cell-face flow rate [L^3/T],

Δc_i is the cell width of row i [L],

$n_{i,j,k}$ is the effective porosity of cell i,j,k, and

$l_{i,j,k}$ is the saturated thickness of unconfined cell i,j,k or thickness of confined cell i,j,k [L].

The cell-face velocities are calculated using an average saturated thickness, instead of the single-cell saturated thickness used in MODPATH, because the original method produces discontinuities in velocity, and thus sensitivity, at cell boundaries. The cell-face flow rate equals conductance multiplied by the head difference across the cell face (McDonald and Harbaugh, 1988, p. 2-12). For the left cell face j-½:

$$Q_{x_{i,j-1/2,k}} = CR_{i,j-1/2,k}(h_{i,j-1,k} - h_{i,j,k}) \tag{C10}$$

$$CR_{i,j-1/2,k} = 2\Delta c_i \frac{T_{i,j-1,k}\, T_{i,j,k}}{T_{i,j-1,k}\Delta r_j + T_{i,j,k}\Delta r_{j-1}} \tag{C11}$$

where

$CR_{i,j-1/2,k}$ is the conductance in the row direction for the material between the center of adjacent cells i,j-1,k and i,j,k [L^2/T],

$h_{i,j,k}$ is the head in cell i,j,k [L],

Δr_j is the cell width of column j [L],

Δc_i is the cell width of row i [L], and

$T_{i,j,k}$ is the transmissivity of cell i,j,k [L^2/T].

Substituting Equation (C10) into Equation (C9) produces:

$$v_{x_{i,j-1/2,k}} = \frac{2CR_{i,j-1/2,k}(h_{i,j-1,k} - h_{i,j,k})}{n_{i,j,k}\Delta c_i \left(l_{i,j-1,k} + l_{i,j,k}\right)} \tag{C12}$$

The partial derivative of the left cell-face velocity with respect to a parameter b is:

$$\frac{\partial v_{x_{i,j-1/2,k}}}{\partial b} = \frac{2}{n_{i,j,k}\Delta c_i} \left[\begin{array}{l} \dfrac{\partial CR_{i,j-1/2,k}}{\partial b} \dfrac{(h_{i,j-1,k} - h_{i,j,k})}{\left(l_{i,j-1,k} + l_{i,j,k}\right)} + \\[2em] CR_{i,j-1/2,k}\left(\dfrac{\left(l_{i,j-1,k} + l_{i,j,k}\right)\left(\dfrac{\partial h_{i,j-1,k}}{\partial b} - \dfrac{\partial h_{i,j,k}}{\partial b}\right) - (h_{i,j-1,k} - h_{i,j,k})\left(\dfrac{\partial h_{i,j-1,k}}{\partial b} + \dfrac{\partial h_{i,j,k}}{\partial b}\right)}{\left(l_{i,j-1,k} + l_{i,j,k}\right)^2} \right) \end{array} \right]$$

$$\tag{C13}$$

where the sensitivities of the conductance term and of the hydraulic heads to the parameters are calculated by MODFLOWP using the sensitivity-equation method. Equation (C13) shows that there are two components that influence the velocity sensitivity. First, there is the effect due to the sensitivity of the cell material to the parameter of interest $\dfrac{\partial CR_{i,j-1/2,k}}{\partial b}$, which will be zero if the parameter is not included in $CR_{i,j-1/2,k}$. Second, there is the effect of the head sensitivity to the parameter $\dfrac{\partial h_{i,j-1,k}}{\partial b}$ or $\dfrac{\partial h_{i,j,k}}{\partial b}$, which may influence the sensitivities in each cell of the grid due to the change in the head distribution from a change in a parameter value anywhere in the grid. The velocity in every cell, therefore, may be at least somewhat sensitive to all of the parameters.

Calculation of Vertical Cell-Face Velocity and Sensitivity at the Top of the Top Layer

The vertical velocity at the top of the top layer is calculated using the net flux across the top of the layer into or out of the model. Taking velocity in the upward direction as being positive, the velocity $v_{z_{i,j,k-1/2}}$ can be expressed as:

$$v_{z_{i,j,k-1/2}} = -\frac{W_{i,j,k}}{n_{i,j,k}} \tag{C14}$$

where

$\quad W_{i,j,k}$ is the net flux across the top of cell i,j,k [L/T], and

$\quad n_{i,j,k}$ is the porosity of layer k.

The sensitivity of the vertical velocity at the top of the top layer of Equation (C14) is obtained by taking the derivative with respect to a general parameter b:

$$\frac{\partial v_{z_{i,j,k-1/2}}}{\partial b} = -\frac{1}{n_{i,j,k}}\frac{\partial W_{i,j,k}}{\partial b} \tag{C15}$$

When more than one type of boundary contributes to the flux across the top of the top layer, then, because the differential and summation functions are linear, the sensitivity of the velocity is equal to the sum of the sensitivity of each of the components.

Calculation of Vertical Cell-Face Velocity and Sensitivities Between Layers

The Vcont conductance is used to calculate the flux between two layers using the head difference across the layer:

$$Q_{i,j,k+1/2} = Vcont_{i,j,k+1/2} \Delta r_j \Delta c_i \left(h_{i,j,k+1} - h_{i,j,k} \right) \tag{C16}$$

Vcont is calculated for the three conditions shown in Figure 2, respectively, as:

$$Vcont_{i,j,k+1/2} = \frac{2 K_{z_{i,j}}}{l_{i,j,k} + l_{i,j,k+1}} \tag{C17a}$$

$$Vcont_{i,j,k+1/2} = \frac{1}{\frac{l_{i,j,k}}{2 K_{zi,j,k}} + \frac{l_{i,j,k+1}}{2 K_{zi,j,k+1}}} \tag{C17b}$$

$$Vcont_{i,j,k+1/2} = \frac{1}{\frac{l_{i,j,k}}{2 K_{zi,j,k}} + \frac{l_{i,j,k+1/2}}{K_{zc}} + \frac{l_{i,j,k+1}}{2 K_{zi,j,k+1}}} \tag{C17c}$$

where

$K_{z_{i,j,k}}$ is the vertical hydraulic conductivity of cell i,j,k [L/T],

$l_{i,j,k}$ is the thickness of layer k [L],

K_{z_c} is the vertical hydraulic conductivity of the confining layer [L/T], and

$l_{i,j,k+1/2}$ is the thickness of the confining layer.

Vcont, a model input, is included in the model arrays by multiplying by the area of the cell:

$$CV_{i,j,k+1/2} = Vcont_{i,j,k+1/2} \Delta r_j \Delta c_i \tag{C18}$$

The velocity between model layers is calculated from the flux between layers by dividing Equation (C16) by the effective area of flow. If the particle is in model layer k, the velocity is:

$$v_{z_{i,j,k+1/2}} = \frac{CV_{i,j,k+1/2} \left(h_{i,j,k+1} - h_{i,j,k} \right)}{n_{i,j,k} \Delta r_j \Delta c_i} \tag{C19a}$$

and if the particle is in model layer k+1 the velocity is:

$$v_{z_{i,j,k+1/2}} = \frac{CV_{i,j,k+1/2} \left(h_{i,j,k+1} - h_{i,j,k} \right)}{n_{i,j,k+1} \Delta r_j \Delta c_i} \tag{C19b}$$

63

If the aquifer conditions in (a) above are being represented, then $n_{i,j,k}$ is probably equal to $n_{i,j,k+1}$.

The sensitivity of the velocities in Equation (C19) are:

$$\frac{\partial v_{z_{i,j,k+1/2}}}{\partial b} = \frac{1}{n_{i,j,k}\Delta r_j \Delta c_i}\left[\frac{\partial CV_{i,j,k+1/2}}{\partial b}\left(h_{i,j,k+1} - h_{i,j,k}\right) + CV_{i,j,k+1/2}\left(\frac{\partial h_{i,j,k+1}}{\partial b} - \frac{\partial h_{i,j,k}}{\partial b}\right)\right] \text{(C20a)}$$

$$\frac{\partial v_{z_{i,j,k+1/2}}}{\partial b} = \frac{1}{n_{i,j,k+1}\Delta r_j \Delta c_i}\left[\frac{\partial CV_{i,j,k+1/2}}{\partial b}\left(h_{i,j,k+1} - h_{i,j,k}\right) + CV_{i,j,k+1/2}\left(\frac{\partial h_{i,j,k+1}}{\partial b} - \frac{\partial h_{i,j,k}}{\partial b}\right)\right]$$

$$\text{(C20b)}$$

With the exception of the different porosity terms and the absence of the saturated thickness term, Equation (C20) is similar to the horizontal cell-face sensitivity in Equation (C13).

Calculation of Particle Displacement and Sensitivity in Layers Separated by a Confining Unit

If adjacent layers are being represented as having a confining layer separating them, then the particle tracking and calculation of sensitivities are more complicated. If Vcont represents a confining unit, it is assumed that flow through the confining layer is vertical (Figure 3). In this case, the x- and y-locations of the particle, and thus their sensitivities, will not change as the particle travels through the confining layer. Because of continuity of flow, the velocity in the model layers above and below the confining layer can be calculated using Equations (C19) above. Particle displacement is calculated using exponential particle tracking. The velocity in the confining layer is calculated as in Equation (C19), but using the porosity in the confining layer $n_{i,j,c}$, as:

$$v_{z_{i,j,k+1/2}} = \frac{CV_{i,j,k+1/2}\left(h_{i,j,k+1} - h_{i,j,k}\right)}{n_{i,j,c}\Delta r_j \Delta c_i} \tag{C21}$$

The time that it takes the particle to travel through the confining unit is calculated using Euler-integration particle tracking:

$$\Delta t_z = \frac{l_{i,j,k+1/2}n_{i,j,c}\Delta r_j \Delta c_i}{CV_{i,j,k+1/2}\left(h_{i,j,k+1} - h_{i,j,k}\right)} \tag{C22}$$

The sensitivity of the vertical velocity within a confining layer of Equation (C21) is:

64

$$\frac{\partial v_{z_{i,j,k+1/2}}}{\partial b} = \frac{1}{n_{i,j,c}\Delta r_j \Delta c_i}\left[\frac{\partial CV_{i,j,k+1/2}}{\partial b}\left(h_{i,j,k+1} - h_{i,j,k}\right) + CV_{i,j,k+1/2}\left(\frac{\partial h_{i,j,k+1}}{\partial b} - \frac{\partial h_{i,j,k}}{\partial b}\right)\right] \quad \text{(C23)}$$

Then the change in the sensitivity of the z-location of the particle to a parameter b is calculated as:

$$\frac{\partial \Delta z}{\partial b} = \frac{\partial v_{z_{i,j,k+1/2}}}{\partial b}\Delta t_z = \frac{\partial v_{z_{i,j,k+1/2}}}{\partial b}\frac{l_{i,j,k+1/2}n_{i,j,c}\Delta r_j \Delta c_i}{CV_{i,j,k+1/2}\left(h_{i,j,k+1} - h_{i,j,k}\right)} \quad \text{(C24)}$$

where, because time is an independent variable, the sensitivity of the time step size $\frac{\partial \Delta t_z}{\partial b}$ is zero .

<div align="center">Correction of Vertical Position for Distorted Grids</div>

The corrected position is calculated using the uncorrected position and thickness and bottom elevation of the respective cells. When the particle moves from column j to column j+1, for example, the correction is calculated as:

$$z^t_{P_{corrected}} = z_{bot_{i,j+1,k}} + \frac{z^t_{P_{uncorrected}} - z_{bot_{i,j,k}}}{l_{i,j,k}}l_{i,j+1,k} \quad \text{(C25)}$$

where

$z^t_{P_{corrected}}$ is the corrected vertical position of the particle at time-step t,

$z^t_{P_{uncorrected}}$ is the uncorrected vertical position of the particle at time-step t, and

$z_{bot_{i,j,k}}$ is the elevation of the bottom of cell i,j,k.

APPENDIX D: PROGRAM DESCRIPTION

Program Description

Hill (1992) uses the terms "primary module" and "submodule" when referring to subroutines in MODFLOWP and that terminology is used in this report. Only modules that were modified from those presented in Hill (1992) or which are new are discussed in this section. For modified modules, only the modifications are discussed.

The modules of the ADV Package are referred to as new in the following discussion and are named with the label ADV; the prefix S is added to indicate submodules that are called by an ADV module. The remaining characters of the module names were assigned according to conventions used by McDonald and Harbaugh (1988) and Hill (1992).

Advective-transport observations are included in a parameter-estimation iteration subsequent to the calculation of the heads by calling the module ADV1P from SEN1OT. ADV1P is the main module, which tracks particles and calculates sensitivities by (1) initializing the coordinates of the particle at the starting position of the observed path of advective transport, (2) tracking the particle through the grid using Equations (3) and (4), and (3) calculating sensitivities using Equations (C1) and (C2). ADV1P calls SADV1L to calculate the linearly-interpolated velocity from the cell-face velocities. ADV1P then calls SADV1S to calculate the semi-analytical particle displacement. When the observation time is reached, the particle tracking is stopped and the final x-, y-, and z-locations and sensitivities of those locations to the parameters are used by the modified Gauss-Newton optimization method in addition to the head and flow observations to update the parameter values. Sensitivities are only calculated if IPAR on LINE 6 of the parameter-estimation input file is set to 0 or 1. The parameter-estimation iterations are continued until changes in the parameter values from one iteration to the next are small enough to satisfy the convergence criteria.

Modified MAIN

Statements are added to initialize variables that may be needed in the ADV Package. Subroutine calls are modified to include variables needed in the ADV Package.

Modified primary modules—listed in order of appearance in MAIN

> SEN1AL   IOUADV is read from position 12 on LINE 7 of the parameter-estimation INPUT FILE and LINE 1 of the ADV INPUT FILE is read to dimension space for the ADV Package.

> SEN1RP   Call to ADV1RP is added to read in particle-tracking information.

> SEN1OT   Call to ADV1P is added to calculate advective-transport observation and sensitivities.

Modified submodules

> SSEN1O   Call ADV1O to print information about the advective-transport observation residuals.

> PAR1RE   Include advective-transport observation residuals in the normality calculation.

New primary modules

> ADV1RP   Reads, checks, prints, and stores information from the ADV INPUT FILE.

> ADV1P   Controls particle tracking by calling SADV1L and SADV1S.

> ADV1O   Print information about the advective-transport observation residuals.

New submodules

> SADV1L   Calculates the linearly-interpolated velocity at any point within a cell from the cell-face velocities and calculates sensitivity of that velocity to the parameters.

> SADV1S   Calculates the semi-analytical particle displacement and sensitivity to parameters.

> SADV1WR   Writes particle-tracking summary information to the main output file and IOUTT2 file, if specified.